

**Sudan University of Science and Technology**  
**College of Graduate Studies**

**Determination of Electron Temperature in the  
Plasma of Alkaline Earth Group Produced by  
Different Lasers, a Computer Simulation**

تحديد درجة حرارة الكثرونات البلازما لمجموعة الفلزات  
الترابية المنتجة بواسطة ليزرات مختلفة, محاكاة حاسوبية

**A thesis submitted for the fulfillment of the requirements for the  
degree of Doctor of Philosophy in Laser Applications in Physics**

By:

**Gehan Abdalla Omer Musa**

Supervised by:

**Prof. Dr. Nafie A. Almuslet**

February /2016

## الآية

بِسْمِ اللّٰهِ الرَّحْمٰنِ الرَّحِیْمِ

( سُرِّيهِمْ آيَاتِنَا فِي الْأَفَاقِ وَفِي أَنْفُسِهِمْ حَتَّىٰ يَبَيِّنَ لَهُم مِّنْهُ الْحَقَّ ۗ أَوَلَمْ

يَكْفِ بِرَبِّكَ أَنَّهُ عَلَىٰ كُلِّ شَيْءٍ شَهِيدٌ )

سورة فصلت الاية 53

# Dedication

To

The soul of my mother, grandmother, uncle

My father

My husband

My brothers and sisters

All those who love science and technology

# Acknowledgements

First, and foremost I thank Allah, who gives me the opportunity and strength to carry out this work.

Second I would like to thank my supervisor, Prof. Nafie A. Almuslet, who has been a constant source of knowledge and guidance over the course of the project. His support and direction has been essential throughout my Ph.D. and I could not have wished for a better supervisor.

Also I would like to extend this gratitude to teacher Sahar Salah Aldeen Mohammed (Teacher Assistant in Faculty of Mathematical Science in University of Khartoum) for creating and running the program.

I would like to extend my thanks to all the staff in Institute of Laser in Sudan University of Science and Technology, for their help, inspiration, and moral support.

I need to send a special thanks to my family for their support and help all the time.

Finally I would like to thank all my colleagues, and all those who helped through the duration of this work.

**Gehan Abdalla Omer Musa**

# Abstract

In this work, a computer simulation was built and operated to simulate the plasma of Alkaline earth group produced by different lasers, Iodine laser at wavelengths of 1.3 $\mu\text{m}$ , and 0.44 $\mu\text{m}$ . Nd-YAG laser with wavelengths of 1.064 $\mu\text{m}$ , 0.532 $\mu\text{m}$  and 0.355 $\mu\text{m}$ . Excimer laser at wavelengths of 0.248 $\mu\text{m}$  and 0.193 $\mu\text{m}$ . Different laser intensities in the range of  $1 \times 10^9 \text{W/cm}^2$  to  $1 \times 10^{13} \text{W/cm}^2$  were used to calculate the electron temperature of the plasma of these elements.

This simulation was depended on the matlab program. The relations between the plasma electron temperature and laser power densities, wavelengths, and atomic numbers of the elements were studied.

It was found that the plasma electron temperature increased when the laser intensities were increased. While the plasma electron temperature increased with increasing the wavelength of the lasers. The relation between the plasma electron temperature and the atomic numbers of the alkaline earth group is inverse relation, when the atomic number increased the plasma electron temperature decreased.

This study recommended to applying this study experimentally to compare the practical results with the simulation results.

## المستخلص

تم فى هذا العمل بناء وتشغيل برنامج محاكاة حاسوبى يحاكي انتاج البلازما من مجموعة الفلزات الترابية بواسطة عدة ليزرات هى ليزر اليود ذى الطولين الموجيين 1.3 مايكروميتر و0.44 مايكروميتر وليزر النيوديميوم - ياق ذى الاطوال الموجية 1.064 مايكروميتر و0.532 مايكروميتر و0.355 مايكروميتر وايضا الاكسايمر ليزر ذى الطولين الموجيين 0.248 مايكروميتر و0.193 مايكروميتر. استخدمت فى هذا العمل كثافات قدرة مختلفة لهذه الليزرات فى المدى من  $10^9 * 1$  واط/سم<sup>2</sup> الى  $10^{13} * 1$  واط/سم<sup>2</sup>.

اعتمد البرنامج الحاسوبى لغة الماتلاب للمحاكاة وصمم لحساب درجة حرارة الكترونات البلازما من مجموعة العناصر اعلاه. وتم دراسة علاقة درجة حرارة الكترونات البلازما المتحصل عليها مع كل من كثافة قدرة الليزرات المستخدمة والطول الموجى لهذه الليزرات والعدد الذرى للعناصر المستخدمة. وجد ان هنالك علاقة بين كثافة القدرة ودرجة حرارة الكترونات البلازما وهى علاقة طردية. كما وجد ان العلاقة بين درجة حرارة الكترونات البلازما والاطوال الموجية هي علاقة طردية اى كلما زاد الطول الموجى لليزر المستخدم كلما زادت درجة الحرارة. واخيرا وجد ان العلاقة بين الاعداد الذرية للعناصر ودرجة حرارة الكترونات البلازما هي علاقة عكسية اى كلما زاد العدد الذرى كلما قلت درجة حرارة البلازما. فى نهاية البحث تمت التوصية بتطبيق هذه الدراسة عمليا للمقارنة بين النتائج العملية والنتائج التى تحصلت عليها هذه الدراسة .

# Table of Contents

Title .....	Page No
الآية.....	I
Dedication.....	II
Acknowledgements.....	III
Abstract .....	IV
المستخلص.....	V
Table of Contents.....	VI
List of Tables.....	XI
List of Figures.....	XII

## Chapter One

### Laser Plasma Interaction, Basic Concepts

1.1 Introduction.....	1
1.2 Aims of the work.....	2
1.3 Structure of the thesis.....	2
1.4 Plasma Parameters.....	2
1.4.1 The Particles Density.....	3
1.4.2 Temperature and Velocity(energy)Distribution function....	3
1.4.3 Debye Length.....	4
1.4.4 Plasma Frequency.....	5
1.4.5 Cyclotron Frequency and Larmor Radius.....	5
1.4.6 Thermal Speed.....	7
1.5 Transport Coefficients in Plasma.....	7
1.5.1 Electrical Conductivity.....	7
1.5.2 Thermal Conductivity.....	8
1.5.3 Diffusion.....	8
1.6 Classification of Plasma.....	9
1.6.1 Cold Plasma.....	9

1.6.2	Hot plasma.....	9
1.7	Plasma Production .....	10
1.7.1	The Glow Discharge.....	10
1.7.2	RF-Produced Plasmas.....	11
1.7.3	Laser produced Plasmas.....	11
1.8	Lasers for Producing Plasma .....	13
1.8.1	X-ray Lasers.....	14
1.9	Atomic Processes in Plasma .....	15
1.9.1	Bound – Bound Processes.....	16
1.9.1.1	Radiative Bound – Bound Processes.....	16
1.9.1.2	Collisional Bound – Bound Processes... ..	17
1.9.2	Bound – Free Processes.....	18
1.9.3	Free – Free Processes.....	20
1.10	Equation of State.....	21
1.11	Fluid Model.....	23
1.11.1	The Concept of Fluid Description .....	24
1.12	Plasma Waves.....	24
1.12.1	Unmagnetized Plasmas.....	25
1.12.2	Magnetized Plasmas.....	26
1.12.3	Thermal Plasmas.....	27
1.12.4	Landau Damping.....	27
1.12.5	Pondermotive Force.....	27
1.13	Shock Waves.....	28
1.13.1	Scaling of Shock Pressure With Laser Intensity.....	29
1.13.2	Shock Velocity.....	31
1.13.3	Coupling Parameter.....	32
1.14	Plasma Industrial Applications.....	32
1.14.1	Semiconductor Electronics.....	32



1.14.2	Plasma Spray.....	33
1.14.3	Plasma Welding, Cutting and Material Processing .....	33
1.14.4	MHD Energy Conversion and Ion Propulsion.....	33
1.14.5	Gas Lasers.....	34
1.15	Theoretical Models for Plasma .....	34
1.15.1	Local Thermodynamic Equilibrium.....	35
1.15.2	Non – LTE .....	36
1.15.3	Coronal Equilibrium (CE).....	37
1.15.4	Collisional Radiative Equilibrium.....	37

## **Chapter Two**

### **Plasma Temperature, Techniques of Measurements and Calculations**

2.1	Introduction .....	39
2.2	Plasma Diagnostic Techniques.....	39
2.2.1	Optical Emission Spectroscopy.....	39
2.2.2	Laser Induced Fluorescence Spectroscopy.....	39
2.2.3	Mass Spectroscopy.....	40
2.2.4	Optical Absorption Spectroscopy.....	40
2.2.5	Langmuir Probe.....	41
2.2.6	Interferometers.....	41
2.2.7	Thomson Scattering.....	41
2.2.8	Shadowgraphy.....	42
2.3	Temperature and Equilibrium .....	42
2.4	Measurement Techniques of Temperature.....	44
2.4.1	The Boltzmann plot Technique.....	44
2.4.2	Temperature from Doppler Profile.....	46
2.4.3	Temperature from Shock waves.....	47
2.5	Literature Review.....	48

**Chapter Three**  
**The Computer Simulation**

3.1	Introduction.....	55
3.2	Modeling Method.....	55
3.3	Numerical Simulation.....	55
3.4	Matlab Program.....	56
3.5	Target materials.....	57
3.6	Lasers Used in the Simulation.....	57
	3.6.1 Nd-YAG laser.....	57
	3.6.2 Excimer laser.....	58
	3.6.3 Iodine Gas laser.....	58
3.7	The Simulation Work.....	59
	3.7.1 Program Input.....	59
	3.7.1.1 Material Parameters.....	59
	3.7.1.2 Laser Parameters.....	59
	3.7.2 Program Output.....	59
3.8	Program Structure.....	59
	3.8.1 The Relation between Electron Plasma Temperature and Lasers Intensities .....	60
	3.8.2 Determination of the Relation between Plasma Electron Temperature and Wavelengths of the Lasers .....	62
	3.8.3 The Relation between Electron Plasma Temperature and Atomic Numbers of the elements.....	63
3.9	The Program Screens.....	64

## Chapter Four

### Results and Discussion

4.1	Introduction.....	72
4.2	The Electron Temperature Deduced with Different Lasers and the Different Lasers Intensities.....	73
4.3	The Relation between the Electron Temperature and Lasers Wavelengths.....	76
4.4	The Results of Electron Temperature Dependence on the Atomic Numbers (Z) of the Alkaline Earth Group.....	79
4.5	The Discussion.....	85
4.5.1	The Electron Temperatures Deduced with Different Lasers and Different Intensities.....	85
4.5.2	The Relation between the Electron Temperature and Lasers Wavelengths.....	86
4.5.3	The Electron Temperature Dependence on the Atomic Numbers (Z).....	89
4.6	Conclusions.....	90
4.7	Recommendations.....	90
	References.....	91

## List of Tables

<b>Title of the Table</b>	<b>Page No.</b>
Table (3-1): The Parameters of the Alkaline Earth Group	57
Table (4-1): The parameters of lasers used in the simulation	72

## List of Figures

Title of the Figure	Page No.
Fig (1-1): The range of temperatures and densities of plasmas	1
Fig (1-2): The debyesheilding	4
Fig (1-3): The electron trajectory in a magnetic field	6
Fig (1-4): Schematic of low pressure glow discharge	10
Fig (1-5): Schematic of an RF discharge	11
Fig(1-6): Schematic diagram of expanding laser produced plasma	12
Fig(1-7): Part of the electromagnetic spectrum, IR is infrared, UV is ultraviolet, VUV is vacuum ultraviolet, extreme ultraviolet is EUV and the X-UV belongs to 3-60 nm	14
Fig (1-8): Schematic illustration of the photoabsorption (left) and spontaneous decay (right) atomic processes which occur in laser produced plasmas. $E_1$ and $E_2$ are lower and upper electron energy states of the atom/ion respectively	17
Fig (1-9): Schematic diagram of the electron impact excitation (left) and electron impact deexcitation (right) atomic processes which occur in laser produced plasmas	18
Fig(1-10): Schematic illustration of the Radiative Recombination (left) and Photoionization (right) atomic processes that occur in laser produced plasmas. $E_1$ , $E_2$ , $E_3 \dots E_n$ are bound electronic states of the atom/ion.	19
Fig (1-11): Schematic diagram of the Bremsstrahlung (left) and Inverse Bremsstrahlung (right) atomic processes that occur in laser produced plasmas	21
Fig(1-12): The ablation pressure	31

Fig (3-1): The Iodine laser system	58
Fig (3-2): Flow chart of the relation between electron plasma temperature with laser intensities	61
Fig (3-3): Flow chart of the relation between electron temperature and wavelength of lasers	62
Fig (3-4): Flow chart of the relation between the electron plasma temperature and atomic numbers of materials	63
Fig (3-5): The two parts of the first screen	64
Fig (3-6): The steps to calculate the pressure of the laser	65
Fig (3-7): The screen explain the pressures equations	66
Fig(3-8): The details of the pressure in the critical layer to calculate the electron temperature and plot the relation between electron temperature and intensities of the laser	67
Fig(3-9): The high pressure with time duration to calculate the electron temperature and plot the relation between electron temperature and intensities of the laser	68
Fig(3-10): The screen used to calculate the electron temperature and plot the relation between electron temperature and intensities of the laser	69
Fig(3-11): The relation between the electron temperature and wavelength of lasers	70
Fig(3-12): The steps to find the relation between electron temperature and atomic numbers of elements	71
Fig (4-1): The relation between T(eV) of Be and lasers intensities ( $W/cm^2$ )	73
Fig (4-2): The relation between T(eV) of Mg and lasers intensities ( $W/cm^2$ )	73
Fig (4-3): The relation between T(eV) of Ca and lasers intensities ( $W/cm^2$ )	74
Fig (4-4): The relation between T(eV) of Sr and lasers intensities ( $W/cm^2$ )	74
Fig (4-5): The relation between T(eV) of Ba and lasers intensities ( $W/cm^2$ )	75
Fig (4-6): The relation between T(eV) of Ra and lasers intensities ( $W/cm^2$ )	75

Fig (4-7): The relation between T (eV) of Be and lasers wavelengths ( $\mu\text{m}$ )	76
Fig (4-8): The relation between T (eV) of Mg and lasers wavelengths ( $\mu\text{m}$ )	76
Fig (4-9): The relation between T (eV) of Ca and lasers wavelengths ( $\mu\text{m}$ )	77
Fig (4-10): The relation between T (eV) of Sr and lasers wavelengths ( $\mu\text{m}$ )	77
Fig (4-11): The relation between T (eV) of Ba and lasers wavelengths ( $\mu\text{m}$ )	78
Fig (4-12): The relation between T (eV) of Ra and lasers wavelengths ( $\mu\text{m}$ )	78
Fig (4-13): The relation between the electron temperature (eV) and the atomic numbers of the elements with different lasers at $1 \times 10^9 (\text{W}/\text{cm}^2)$	79
Fig (4-14): The relation between the electron temperature (eV) and the atomic numbers of the elements with different lasers at $3 \times 10^9 (\text{W}/\text{cm}^2)$	79
Fig (4-15): The relation between the electron temperature (eV) and the atomic numbers of the elements with different lasers at $6 \times 10^9 (\text{W}/\text{cm}^2)$	80
Fig (4-16): The relation between the electron temperature (eV) and the atomic numbers of the elements with different lasers at $1 \times 10^{10} (\text{W}/\text{cm}^2)$	80
Fig (4-17): The relation between the electron temperature (eV) and the atomic numbers of the elements with different lasers at $3 \times 10^{10} (\text{W}/\text{cm}^2)$	81

Fig (4-18): The relation between the electron temperature (eV) and the atomic numbers of the elements with different lasers at $6 \times 10^{10} (\text{W}/\text{cm}^2)$	81
Fig (4-19): The relation between the electron temperature (eV) and the atomic numbers of the elements with different lasers at $1 \times 10^{11} (\text{W}/\text{cm}^2)$	82
Fig (4-20): The relation between the electron temperature (eV) and the atomic numbers of the elements with different lasers at $3 \times 10^{11} (\text{W}/\text{cm}^2)$	82
Fig (4-21): The relation between the electron temperature (eV) and the atomic numbers of the elements with different lasers at $6 \times 10^{11} (\text{W}/\text{cm}^2)$	83
Fig (4-22): The relation between the electron temperature (eV) and the atomic numbers of the elements with different lasers at $1 \times 10^{12} (\text{W}/\text{cm}^2)$	83
Fig (4-23): The relation between the electron temperature (eV) and the atomic numbers of the elements with different lasers at $3 \times 10^{12} (\text{W}/\text{cm}^2)$	84
Fig (4-24): The relation between the electron temperature (eV) and the atomic numbers of the elements with different lasers at $6 \times 10^{12} (\text{W}/\text{cm}^2)$	84
Fig (4-25): The relation between the electron temperature (eV) and the atomic numbers of the elements with different lasers at $1 \times 10^{13} (\text{W}/\text{cm}^2)$	84



# Chapter One

## Laser Plasma Interaction, Basic Concepts

### 1.1 Introduction

The plasma state is a gaseous mixture of positive ions and electrons. Plasmas can be fully ionized, as the plasma in the sun, or partially ionized, as in fluorescent lamps, which contain a large number of neutral atoms (Piel,2010).

Matter in the plasma state can range in temperature from hundreds of thousands of electronvolts ( $1 \text{ eV} = 11,605^\circ \text{ absolute}$ ) to just 100th of an electronvolt. In density, plasmas may be tenuous, with just a few electrons present in a million cubic centimeters, or they may be dense, with more than  $10^{20}$  electrons packed per cubic centimeter fig(1-1).

Plasmas are prodigious producers of electromagnetic radiation. (Peratt, 2015).

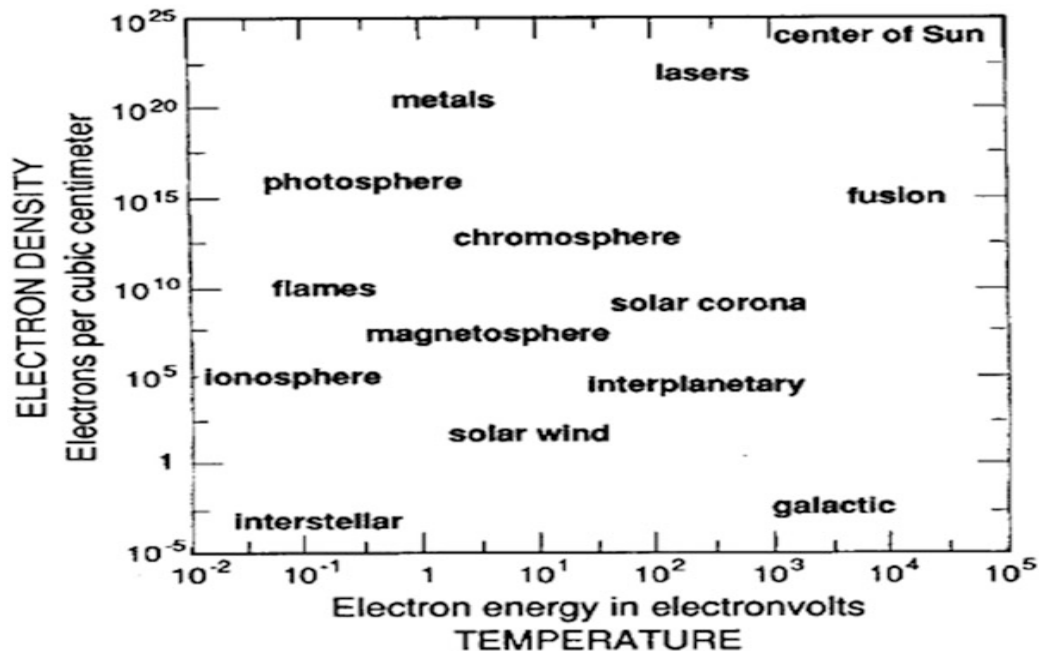


Fig (1-1): The range of temperatures and densities of plasmas

## **1.2 Aims of the work**

The aims of this study are to determine the plasma temperature and related factors in the plasma of the Alkaline earth Group (Be, Mg, Ca, Sr, Ba, Ra) by computer simulation using several types of lasers with different intensities, and to calculate the electron temperature of this group and to find the relation between the plasma electron temperature and the wavelengths of the lasers and atomic numbers of these elements.

## **1.3 Structure of the Thesis**

The basic concepts of plasma, plasma parameters, and laser produced plasma, and industrial applications of plasma are described in the first chapter of this thesis. Chapter two covered the measurements and calculations of plasma temperature and literature review. In chapter three, detailed description of the numerical simulation of plasma temperature, the target materials, and the lasers used in simulation, are given. Chapter four deals with the results of the simulation of the laser produced plasma and the calculation of the plasma temperature. Also this chapter discusses the relation between plasma temperature and wavelengths of the lasers, and atomic numbers of targets. At the end of this chapter, conclusions and future work are presented.

## **1.4 Plasma Parameters**

Plasma is a much more complicated medium, and various important characteristic lengths and characteristic frequencies exist.

Three fundamental parameters characterize plasma:

1. The Particles density  $n$  (measured in particles per cubic meter).
2. The Temperature  $T$  of each species (usually measured in eV, where  $1 \text{ eV} = 11\ 600 \text{ K}$ ).

3. The steady-state magnetic field  $B$  (measured in Tesla).

For partially ionized plasmas, the fractional ionization and cross-sections of neutrals is also important (Bellan, 2004).

### 1.4.1 The Particles Density

The density of each species in plasma is the first important parameter, and among these, the electron and ion densities are the most important. The number density  $n_j$  ( $j = e, i$ ) rather than the mass density  $\rho_j (\equiv m_j n_j)$  is more commonly used, and this quantity is frequently called simply the density. In some plasma, there are multiple-ionized ions, and the density of each ionized state may be important. There are also cases when negative ions, formed by the attachment of electrons to atoms and molecules, can be important in determining plasma behavior. The difference between ion and electron densities gives the space charge  $\sigma = e(n_i - n_e)$  (the ions are assumed to be singly ionized). Another important parameter is the plasma current density  $j = (n_i v_i - n_e v_e)$ , where  $v_i$  and  $v_e$  are the average ion and electron velocities, respectively (Muraoka, 2001).

### 1.4.2 Temperature and velocity (energy) distribution function

The most important parameter related to particle transport and motion is the temperature, but it should be noted that there are many plasmas in which there is a large difference between the temperatures of the electrons and ions, and a large difference in their response to electromagnetic fields. This is due to the fact that the ions and electrons are not in energy equilibrium in many plasma conditions. This can be understood by considering the equation of motion for the charged particle species in an electromagnetic field:

$$m_j \frac{\partial v_j}{\partial t} = q_j (E + v_j \times B) \quad (1.1)$$

Where  $E$ ,  $B$ ,  $V$ ,  $m$  and  $q$  are electric and magnetic field, particle velocity, mass and charge, respectively,  $j = e, i$ . The electron acceleration due to the fields is much larger than the ion acceleration, because  $m_e \ll m_i$  and  $q_e \sim q_i$ . In addition, although the rate of energy transfer is large for the case of electron–electron collisions and ion–ion collisions, the energy exchange in an electron–ion collision is of the order of  $m_e / m_i$ . Because of this, there are many plasmas in which the electron and the ion groups are at different thermal equilibria. In these cases, two temperatures, called the electron temperature and the ion temperature are defined separately (Muraoka, 2001).

### 1.4.3 Debye Length

One of the fundamental properties of plasma is the distance over which the electric field from such a charge is shielded (fig (1-2)). This distance is known as the Debye length,  $\lambda_D$ , and is given by:

$$\lambda_D = \sqrt{\frac{\epsilon_0 k T_e}{e^2 n_e}} = 7.43 \times 10^3 \sqrt{\frac{T_e}{n_e}} \text{ (m)} \quad (1.2)$$

Where  $\epsilon_0$  is the permittivity of free space,  $K_B$  is the Boltzmann constant,  $T_e$  is the electron plasma temperature (in kelvin),  $e$  is the electron charge and  $n_e$  is the electron density.

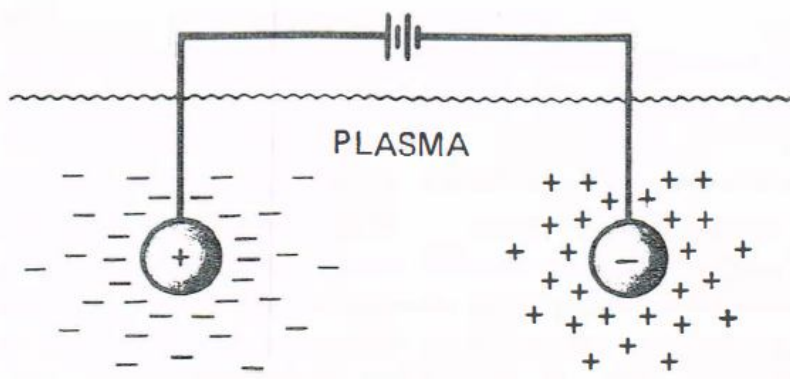


Fig (1-2): The debyesheilding

An extension of the Debye length is the Debye sphere, i.e. the sphere with a radius equal to the Debye length, outside which the electric field of the enclosed charge is zero (fully shielded). The number of electrons,  $N_{De}$ , inside the Debye sphere is then given by:

$$N_{De} = \frac{4\pi n_e}{3} \lambda_D^3 \quad (1.3)$$

A perturbation of a charged particle in the plasma (by e.g., displacing it from its equilibrium position) will immediately affect its neighbors. This collective response of charged ions and/or electrons is an important defining characteristic of a plasma and pertains only when the length of the plasma is considerably greater than the debyelength,  $L \gg \lambda_D$  (Hoigh, 2010).

#### 1.4.4 Plasma Frequency

The plasma frequency is the oscillation frequency of simple unmagnetized plasma when the charge distribution is locally perturbed from its equilibrium, and is given for electrons by:

$$\omega_{pj} = \sqrt{\frac{n_j e^2}{m_j \epsilon_0}} \quad (1.4)$$

where  $j = e, i$ . For laser measurements, the electron plasma frequency is particularly important, and this is given by:

$$\omega_{pe} = 56.3 \sqrt{n_e} \quad (\text{rad s}^{-1}) \quad (1.5)$$

The plasma frequency plays an important role in almost all plasma processes (Swanson, 2003).

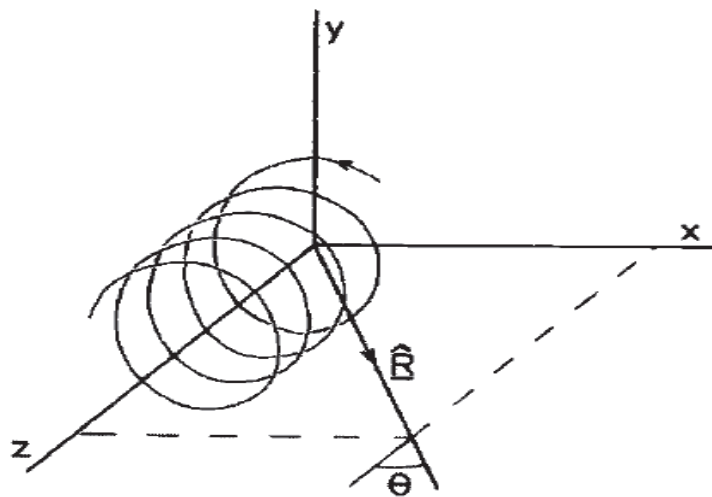
#### 1.4.5 Cyclotron Frequency and Larmor Radius

The motion of charged particles in a plasma can be found by solving the equation of motion (1.1). When a charged particle moves in a

magnetic field (Fig. 1-3), it is convenient to separate the motion into two components, one corresponding to circular motion around the magnetic field (B) and one corresponding to the motion of the centre of the rotation. The rotational component is called cyclotron motion, due to its similarity to the motion of charged particles in a cyclotron accelerator, and the other component is called drift motion. The frequency ( $\omega_{cj}$ ) and radius ( $r_{Lj}$ ) of the cyclotron motion are called the cyclotron frequency  $\omega_c$  and the Larmor radius  $r_L$  respectively. The cyclotron motion of electrons and ions are quite different, due to the large difference in their masses. The values of  $\omega_c$  and  $r_L$ , are very different as is the direction of rotation (Muraoka, 2001). The relevant values of  $\omega_c$  and  $r_L$  (where  $j=i, e$ ) are given by:

$$\omega_{cj} = \frac{eB}{m_j} \text{ (rad s}^{-1}\text{)} \quad (1.6)$$

$$r_{Lj} = \frac{v_j}{\omega_{cj}} \text{ (m)} \quad (1.7)$$



Fig(1-3): The electron trajectory in a magnetic field

#### 1.4.6 Thermal Speed

We define the thermal speed to be the most probable speed in a Maxwellian distribution (Swanson, 2003). The particles in plasma that have temperature  $T_{move}$  with an average speed, related to that temperature, and called the thermal speed. Even if electrons, ions, atoms and molecules have the same temperature, their thermal velocities are quite different because of the large differences in mass (Chen, 1984). The thermal speeds  $v_{th}$  are given by:

$$v_{thj} = \sqrt{\frac{3kT_j}{m_j}} \quad (1.8)$$

## 1.5 Transport Coefficients in Plasma

### 1.5.1 Electrical Conductivity

The definition of the electrical conductivity is given by:

$$j_e = -n_e e v_e = \sigma_E E \quad (1.9)$$

where  $v_e$  is the electron velocity,  $j_e$  is the electric current,  $n_e$  is the electron density and  $\sigma_E$  is the electric conductivity. The relation between the electric current and the electric field is known as Ohm's law. The electrical conductivity is equal:

$$\sigma_E = \frac{n_e e^2}{m_e v_{ei}} [s^{-1}] \quad (1.10)$$

$$\sigma_{E(ei)} = 2.7 * 10^{17} Z \left( \frac{T_e}{\text{KeV}} \right)^{3/2} [s^{-1}] \quad (1.11)$$

Where the electron temperature is in keV, and  $Z$  is the atomic number (Eliezer, 2002).

### 1.5.2 Thermal Conductivity

Consider a medium in which the temperature is not uniform, i.e.  $T$  is a function of space  $T = T(r)$ . The tendency to reach equilibrium requires a flow of heat from the region of higher temperature to that of lower temperature. Defining  $q_H$  as the energy crossing a unit area per unit time in the direction orthogonal to this area, the heat flux (in  $\text{erg}/(\text{cm}^2 \text{ s})$ ) can be defined by:

$$q_H = -\kappa \nabla T \quad (1.12)$$

The value of  $\kappa$  can be easily estimated in a simple model (Eliezer et al., 1986).

### 1.5.3 Diffusion

In equilibrium, the electrons are distributed uniformly throughout the plasma so that  $n_e$  is independent of position. Suppose that a disturbance causes the electron density to depend on position  $n_e(r)$ . In this case the electrons will move in such a way as to restore equilibrium. This motion is described by the diffusion equation:

$$\frac{\partial n_e}{\partial t} = \nabla \cdot (D \nabla n_e) \quad (1.13)$$

where  $D$  is the diffusion coefficient, defined by the relation:

$$j_n = -D \nabla n \quad (1.14)$$

$j_n = n v$  is the particle current density (Eliezer 2002).

## 1.6 Classification of Plasma



Plasmas are characterized by their electron energy  $kT_e$  and their electron density  $n_e$ , several kinds of plasmas in nature and in laboratories. Plasmas can be broadly classified into cold plasmas and thermal plasmas based on the electron energy and electron density.

### **1.6.1 Cold Plasma**

Cold Plasma such as that, which can be obtained by a direct current glow discharge, can also be generated by a high frequency or a microwave discharge at low pressure. In this plasma, the degree of ionization is typically only  $10^{-4}$ , so the gas consists mostly of neutral but excited species. A characteristic feature of this plasma is the lack of thermal equilibrium between the electron temperature and the gas temperature. Hence, this type of plasma is called nonequilibrium plasma. In plasmas generated by discharge under a pressure of less than several tens of torr, the electron temperature becomes high but the gas particles remain at relatively low temperature. This is because the collision frequency between electrons and gas particles is small(HarilaL, 1997).

### **1.6.2 Hot Plasma**

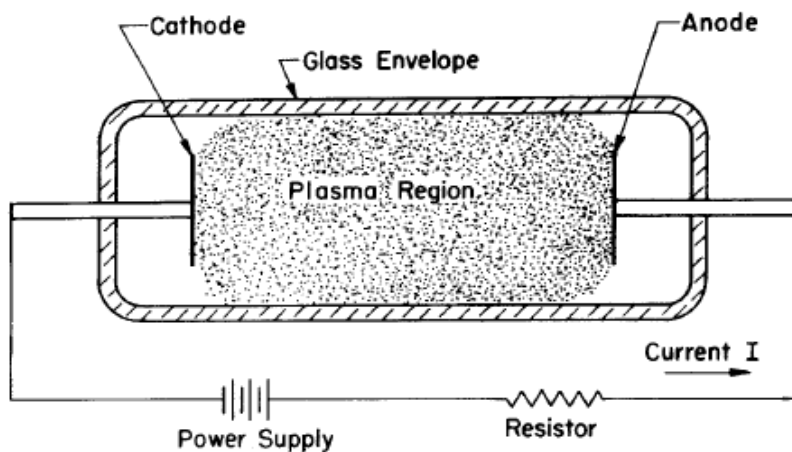
In the plasma generated by an arc discharge, the energy distribution of electrons (characterized by  $T_e$ ) and gas molecules (characterized by  $T_g$ ) are nearly the same, because the collision frequency between electrons and gas molecules becomes large. The plasma is at thermal equilibrium, therefore  $T_e \cong T_g$ . Thermal equilibrium is also reached within each Category of energy states of the gas molecules. Plasma composed of high-temperature gas particles is called thermal plasma (HarilaL, 1997).

## **1.7 Plasma Production**

There are many plasma –production schemes used to produce plasmas for laboratory studies can be described:

### 1.7.1 The Glow Discharge

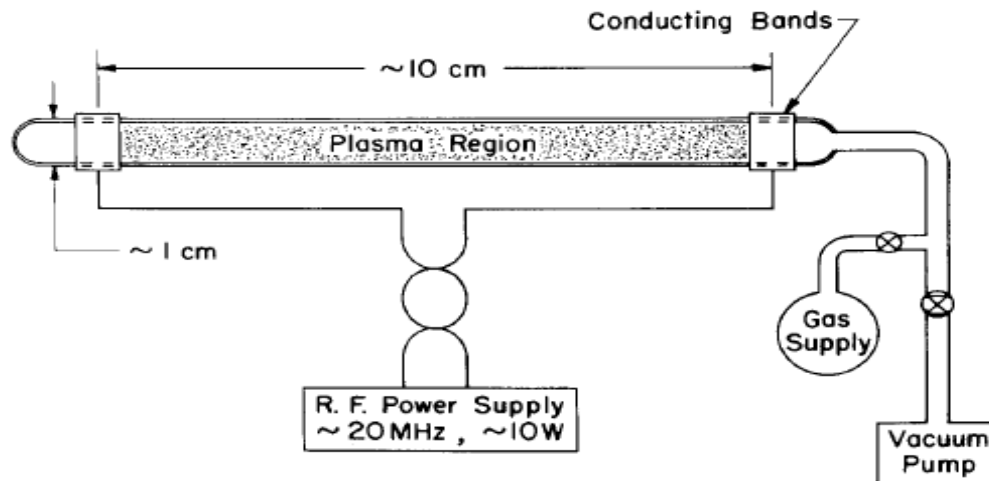
There are many well-established uses of plasma generated by an electric discharge. In principle, discharges can be simply viewed as two electrodes inserted into a glass tube and connected to a power supply. The tube can be filled with various gases or evacuated. As the voltage applied across the two electrodes increases, the current suddenly increases sharply at a certain voltage characteristic of an electron avalanche. If the pressure is low (of the order of a few torr) and the external circuit has a large resistance to prohibit a large current flow, a glow discharge develops fig(1-4). This is a low-current, high-voltage device in which the gas is weakly ionized plasma. Widely used, glow discharges are a very important type of discharge: they form the basis of fluorescent lighting (Fridman, *et al.*, 2004).



Fig(1-4): Schematic of low pressure glow discharge

### 1.7.2 RF-Produced Plasmas

A gas at low pressure will breakdown under the action of an applied steady electric field. It will also breakdown and form a plasma if the applied electric field is altering fig (1-5) illustrate that. The alternating electric field penetrates the dielectric of the glass vessel with no difficulty and accelerates electrons in the vessel to energies above the ionization and recombination usually is only a few percent of the background neutral-gas density. Sometimes RF-produced plasma is created in a magnetic field. These are called cyclotron resonance plasmas when the exciting Rf field has the same frequency for the electrons. Even with the modest Rf power available from microwave sources, plasmas with plasma temperatures in the 20-kev range can be produced by this method (Krall and W,A 1973).



Fig(1-5):Schematic of an RF discharge

### 1.7.3 Laser Produced Plasma

Plasma produced by laser ablation of a solid target takes the form of a plume which expands rapidly away from the target surface. Large spatial gradients in plasma parameters exist along the length of the plume. For example, the densities generally decrease approximately exponentially with distance from the target surface. These variations

in plasma conditions enable a wide range of different phenomena to occur at different positions within the plume. Lifetimes of laser-produced plasmas are typically short, slightly longer in duration than the applied laser pulse. As a result, such plasmas are transient in nature with rapidly evolving hydrodynamics. The combination of rapid plasma evolution and large spatial gradients mean that making experimental measurements suitable for interpreting the plasma behaviour is challenging. Computer simulation of these plasmas is important in order to gain understanding of the processes which occur and to assist interpretation of experimental results (Hall, 2006).

Fig (1-6) showed the expanding laser produced plasma in ambient gas. Plasma plume is divided into many zones having high – density hot and low – density cold plasma. The farthest zone from the target has minimum plasma density and temperature. Laser is absorbed in low – density corona (Singh and Thakur, 2007).

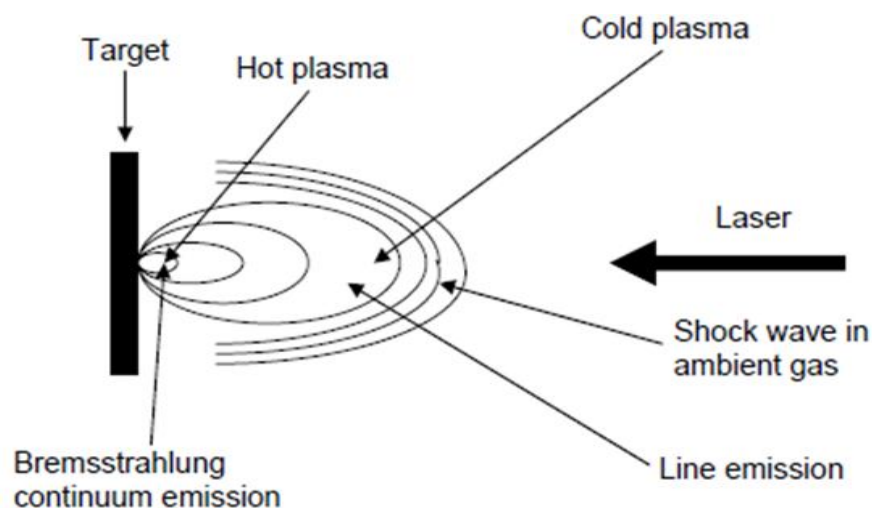


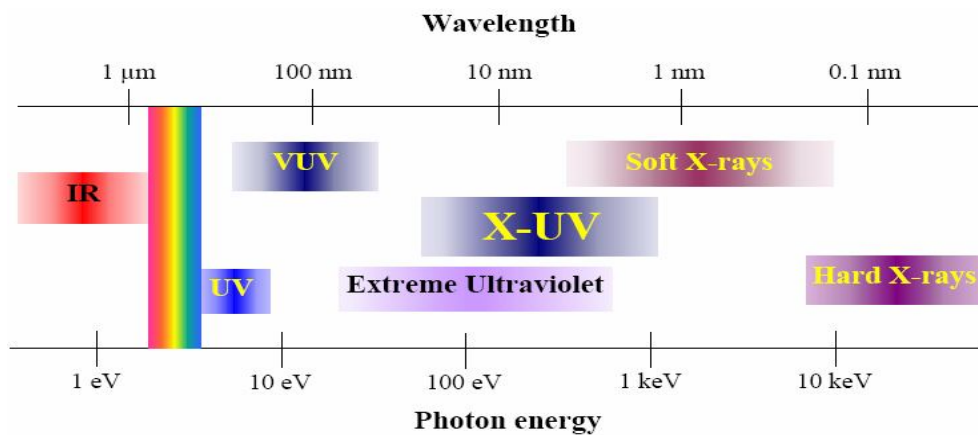
Fig (1-6): Schematic diagram of expanding laser produced plasma

## 1.8 Lasers for Producing Plasma

The word “laser” stems from Light Amplification by Stimulated Emission of Radiation. Light in the form of photons can be absorbed as well as it can be emitted by an atom (Schweitzer, 2008). The main properties of laser light which distinguish it from conventional light sources are the intensity means Lasers are unique sources of high irradiance light required to generate the laser plasma. The unit of irradiance is  $\text{W cm}^{-2}$ , directionality is The ability of the laser pulse to propagate over long distances as a collimated beam. Monochromaticity means that when the Conventional light sources are spectrally broadband, light generating over a wide range of wavelengths (Cremers and Radziemski, 2013). In addition, the laser may operate to emit radiation continuously or it may generate radiation in short pulses. Some lasers can generate radiation with the above mentioned properties and that is tunable over a wide range of wavelengths. Generally pulsed lasers are used in the production of plasmas and also in laser induced breakdown spectroscopy (LIBS). We consider only those properties of lasers relevant to plasma production in gaseous, liquid and solid. It is possible to generate short duration laser pulses with wavelengths ranging from the infrared to the ultraviolet, with powers of the order of millions of watts. Several billions to trillions of watts and more have been obtained in a pulse from more sophisticated lasers. Such high-power pulses of laser radiation can vaporize metallic and refractory surfaces in a fraction of a second. It is to be noted that not only the peak power of the laser, but also the ability to deliver the energy to a specific location is of great importance. The next property of laser radiation that is of interest is the directionality of the beam (Singh and Thakur, 2007).

### **1.8.1 X-Ray Lasers**

X - Ray plasma radiation is a very important addition to spectral measurements in the visible and ultraviolet ranges fig (1-7) explained the part of the electromagnetic spectrum. The name “X ray radiation” is connected with a photon spectral wavelength which is shorter than  $50 \text{ \AA}$ , which corresponds to a photon energy greater than, approximately, 250 eV. The photon energy of soft X rays is less than 100 keV. The first soft X ray radiation investigations in plasma physics, when the solar corona X ray radiation was visualized. The plasma radiation spectrum usually consists of two components, one is continuous and another is a line spectrum. The continuous radiation consists of bremsstrahlung and recombination radiation. Up to the time when laboratory plasma temperatures were not greater than 100 eV the possibility of experimental investigations of plasma X - ray radiations was very limited (Kikuchi et al., 2012).



Fig(1.7) Part of the electromagnetic spectrum, IR is infrared, UV is ultraviolet, VUV is vacuum ultraviolet, extreme ultraviolet is EUV and the X-UV belongs to 3-60 nm

X-ray regime radiation is important because at these wavelengths water becomes transparent and that facilitates the probing of living organisms (Dendy, 1993). The study of radiation damage to biological

cells, the study of the biochemistry of DNA damage and repair are also potential application areas for x-ray.

The medium for an X-ray laser is hot plasma. This hot plasma is created by very powerful existing lasers with an infrared or visible wavelength. Atoms possessing many electrons are ionized and a population inversion is established in this plasma. After the powerful laser creating the plasma had stopped its irradiance, the plasma suddenly cooled down. During the plasma formation or the cooling-down process (due to collisions between the atoms), a population inversion was established and X-ray lasing was observed. The novelty of this laser scheme is that the medium is

plasma, whereas the media for existing lasers are solid, liquid, or gases (Eliezer and Eliezer, 2001). Some of the potential and realized applications possible with x-ray lasers are x-ray lithography, x-ray spectroscopy, x-ray microscopy, scanning and holographic microscopy, the interferometric probing of long lengths of high density laser-plasmas, such as inertial confinement fusion research, the production of high energy particles and gamma rays (Y, 2006).

## **1.9 Atomic Processes in Plasmas**

Many atomic processes occur in plasmas. These processes commence at the instant that the laser radiation impinges on the target surface creating the plasma, right through to plasma expansion and eventual dissipation into the surrounding environment.

When the laser strikes the target, the laser photons can be:

- absorbed by atoms and ions promoting them into excited states (Photo absorption)
- Absorbed by atoms and ions resulting in the liberation of electrons into the free-electron continuum (photoionization).

- Absorption by free electrons in the vicinity of ions which results in an increase in kinetic energy of the electrons (inverse-Bremsstrahlung).

After creation of the plasma with the laser, collisional processes (e.g. excitation, recombination) occur in the plasma for the remainder of its life. They are divided into 3 main types of processes, Bound – Bound (B – B), Bound – Free (B – F) and Free – Free (F-F) (Salzmann, 1998).

### **1.9.1 Bound - Bound Processes**

#### **1.9.1.1 Radiative Bound-Bound Processes**

There are two situations where bound to bound transitions can occur. Firstly, a bound to bound transition can occur in atoms/ions which have an electron dropping from an excited state to one with lower energy releasing a photon in the process. The energy of the liberated photon is equal to the energy difference of the electron before and after the transition. This process is denoted as Spontaneous Decay (Salzmann, 1998) and analysis of the emitted line spectra is important in many plasma diagnostic techniques. Spontaneous decay can be described by:



Where  $A^*$  denotes the atom/ion in an excited state,  $A$  represents the atom/ion in a lower energy state and  $\beta$  represents the photon released during the transition. Conversely a bound to bound transition can also occur when a photon is absorbed by an electron in a low energy state that is consequently promoted to a state of higher energy. In this case the energy difference of the electron before and after its transition is equal to that of the energy of the photon absorbed. This process is denoted as Photo absorption and can be described by:





Where A, A\* and  $\beta$  are as indicated above in equation (1.15). Fig (1-8) depicts these two processes schematically:

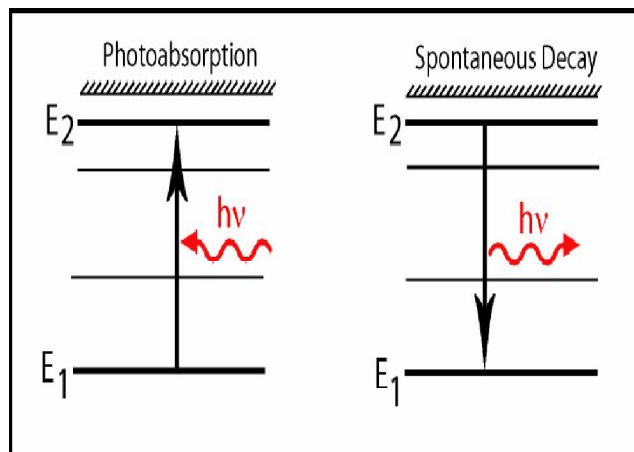


Fig (1-8): Schematic illustration of the photo absorption (left) and spontaneous decay (right) atomic processes which occur in laser produced plasmas.  $E_1$  and  $E_2$  are lower and upper electron energy states of the atom/ion respectively

### 1.9.1.2 Collisional Bound – Bound Processes

In collisional bound – bound processes a bound electron can gain or lose energy i.e., become excited or de-excited after a collision with free electron. Electron Impact Excitation occurs when some or all of the kinetic energy of a free electron is transferred to a bound electron exciting it to a higher energy level (Salzmann, 1998). The energy gained by the bound electron is equal to the energy lost by the free electron. Conversely, Electron Impact De-excitation occurs when a bound electron in an excited state loses energy and is demoted to a state of lower energy upon collision of the host atom or ion with (usually) a free electron. The kinetic energy of the free electron will

be increased by the same amount or quantum of energy that lost by the bound electron in the collision. The balance equation for these collisional bound to bound processes is given in equation (1.17)

$$A + e(\epsilon_1) \leftrightarrow A^* + e(\epsilon_2) \quad (1.17)$$

where  $e$  denotes the free electron,  $A^*$  denotes the atom/ion in an excited state,  $A$  represents the atom/ion in a lower energy state and  $\epsilon_1$  and  $\epsilon_2$  denote the free electron kinetic energies before and after the collision respectively. Also  $\epsilon_1 > \epsilon_2$ . Reading equation (1.17) from the left-hand side to the right-hand side describes the process of electron-impact excitation, and vice-versa for the case of electron-impact de-excitation (Right-to-left).

Fig (1-9) is a simple schematic diagram of the collisional bound – bound atomic processes (Hoigh, 2010),(Salzmann, 1998).

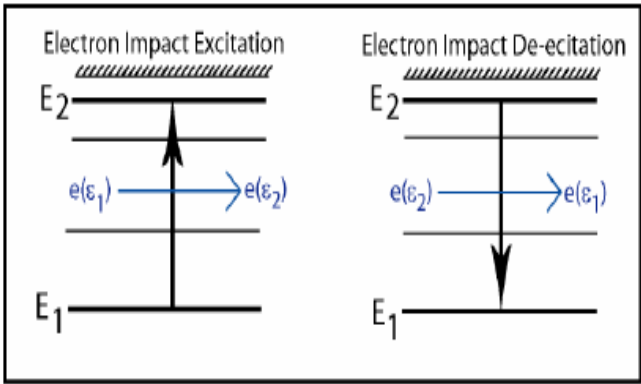


Fig (1-9): Schematic diagram of the electron impact excitation (left) and electron impact de excitation (right) atomic processes which occur in laser produced plasmas

**1.9.2 Bound – Free Processes**

Bound - free transitions also occur in two ways. First of all when a free electron is in the vicinity of an ion, it can be captured by the ion and consequently recombine with the atom. During the process a

photon is released with energy equal to the energy difference of the electron before and after the transition. This process is called Radiative Recombination (RR) (Eliezer, 2002) and can be described by:



where  $e$  is the free electron,  $A^{z+1}$  and  $A^z$  represents ions in charge state  $z+1$  and  $z$  respectively and  $\gamma$  is the emitted photon. The inverse process to Radiative Recombination is the famous photoelectric effect or so called Photoionization (Eliezer, 2002). In photoionization, the absorption of a photon by a bound electron results in the release of the electron into the continuum. The photoelectric is described by:



Where  $e$ ,  $A^{z+1}$ ,  $A^z$ , and  $\beta$  are as already defined. Fig(1-9) illustrates the two bound to free processes.

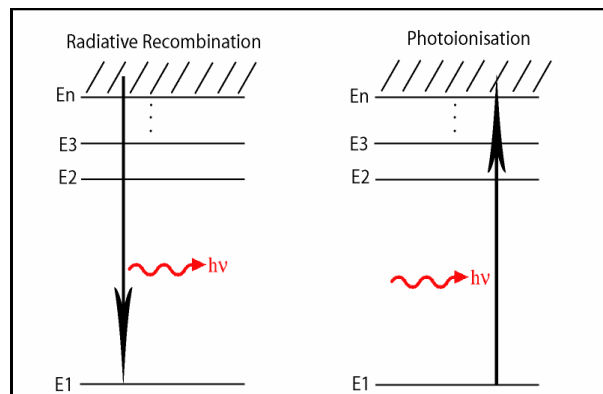


Fig (1-10): Schematic illustration of the Radiative Recombination (left) and Photoionization (right) atomic processes that occur in laser produced plasmas.  $E_1, E_2, E_3 \dots E_n$  are bound electronic states of the atom/ion

### 1.9.3 Free – Free Processes

When a free electron (in the vicinity of a heavy ion) absorbs a photon the kinetic energy of the electron is increased by the quantum of energy absorbed. Because the electron is in the vicinity of the heavy ion, momentum is conserved. This process is called Inverse Bremsstrahlung (IB) and plays a major role in laser radiation absorption by plasma. Inverse Bremsstrahlung is described by (Eliezer, 2002).

$$e(\varepsilon_1) + A + \beta \rightarrow A + e(\varepsilon_2) \quad (1.20)$$

where  $e$  is the free electron,  $\varepsilon_1$  and  $\varepsilon_2$  are the energies of the free electron before and after the process,  $A$  represents the ion and  $\beta$  is the photon. The inverse Bremsstrahlung process is shown schematically below in fig (1-6). The corresponding free – free emission process is known as Bremsstrahlung. Bremsstrahlung or ‘braking radiation’ occurs when an electron is passing through the electric field of an ion (in fact it can happen when passing through any electric field, but for the case of plasmas the field originates from the Coulombic field of an ion in the plasma). The electron may be accelerated in the electric field and thereby emit a photon. Bremsstrahlung can be described by:

$$e(\varepsilon_1) + A \rightarrow e(\varepsilon_2) + A + \beta \quad (1.21)$$

Where  $e$ ,  $\varepsilon_1$ ,  $\varepsilon_2$ ,  $A$ , and  $\beta$  are defined above. Fig(1-11) shows the Bremsstrahlung process schematically.

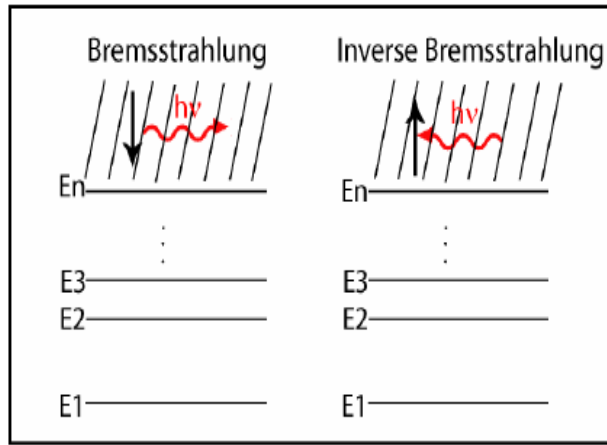


Fig (1-11): Schematic diagram of the Bremsstrahlung (left) and Inverse Bremsstrahlung (right) atomic processes that occur in laser produced plasmas

## 1.10 Equation of State

The equation of state (EOS) describes a physical system by the relation between its thermodynamic quantities, such as pressure, energy, density, entropy, specific heat, and is related to both fundamental physics and the applied sciences. The knowledge of EOS is necessary to understand the science of extreme concentration of energy and matter, behaviour of systems at high pressure, phase transitions, strongly coupled plasma systems, etc. The knowledge of EOS is required for many applications such as inertial fusion energy, astrophysics, geophysics and planetary science, new materials including Nano-particles.

The EOS describes nature over all possible values of pressure, density and temperatures where local thermodynamic equilibrium can be sustained (McKenna et al., 2013). The equation of state plays a crucial role in the hydrodynamics motion of the plasma and it is also closely related to ionization processes. The particular choice of the EOS for equilibrium plasma will give, due to thermodynamic consistency

considerations, a constraint on the temperature-density dependence of the ionization state. The simplest EOS can be derived using the assumption that electrons and ions give independent contributions to the plasma pressure and energy. In other words, the interaction between these two subsystems is neglected in this approximation. The total plasma pressure is therefore the sum of the pressure due to the electron gas and that due to the gas. It can be shown that, for plasma temperatures above 10eV, the electron contribution to the plasma pressure is dominant over the ion one. The plasma pressure is therefore determined by the electron gas pressure and, in the limit of the partially ionized ideal-plasma; one obtains the EOS given by eq(1.22). It has been shown that this choice is consistent with an ionization model which can be interpreted as a simplified version of the saha equation, where only ground –state ions are taken into account (Gizzi, 1994).

$$P \cong P_e = n_e K_B T_e \quad (1.22)$$

In the study of laser interaction with plasmas one often deals with wave-like phenomena such as electromagnetic, electron and ion waves. One can determine which transformation applies to the particular circumstance by comparing the propagation velocity of the particular circumstance by comparing the propagation velocity of the wave with the electron thermal velocity. If  $\omega/k \ll v_{th}$ ,  $\omega$  and  $k$  being the frequency and wave – number of the wave respectively,  $v_{th} = \sqrt{k_B T_e / m_e}$  being the electron thermal velocity.  $T_e, K_B, m_e$  being the electron temperature, the Boltzmann constant and the electron mass respectively, then the plasma undergoes an isothermal transformation and eq(1.21) reduces to:

$$P_e = Cn_e \quad (1.23)$$

$C = K_B T_e$  being constant. On the contrary, when heat flow can be neglected as in the case of  $k \gg v_{th}$ , then an adiabatic transformation takes place and the relation between the density becomes :

$$P_e = Cn_e^\gamma \quad (1.24)$$

$C$  being constant and  $\gamma$  being the ratio of the specific heats,  $C_p/C_v$  given by:

$$\gamma = (2 + N)/N \quad (1.25)$$

For particles with  $N$  degrees of freedom (Osman, 2011). In fully ionized plasma  $\gamma = \frac{5}{3}$ ,  $C_p$  is defined by the specific heat at a constant pressure and  $C_v$  specific heat at a constant volume. The degree of freedom of the system  $N_{free}$ . In one dimension,  $N=1$  and  $\gamma = 3$ , while in three dimensions  $N=3$  and  $\gamma = 5/3$  for free moving particle.

## 1.11 Fluid Model

### 1.11.1 The Concept of Fluid Description

There is one essential difference between hydrodynamics and plasma fluid models. In hydrodynamics, the molecules of the liquid are strongly coupled. This means that the molecules are continuously colliding with their neighbors. A pair of particles will only slowly drift apart by diffusion. Hence, it is meaningful to partition the liquid into macroscopic fluid elements, which contain many molecules that stay close together for a long time. These fluid elements move along streamlines of the flow pattern. For the macroscopic quantities such as density, temperature, and pressure, a simplified fluid picture of the plasma often suffices. For many applications, no charge separation

occurs over the length scales of concern in these cases the plasma can be considered as a single – component fluid. To obtain the simplest one component fluid description, one basically considers statistical averages over the velocity distribution. In hydrodynamics, the description of fluids is based on the three conservation laws of mass, momentum, and energy, resulting in a set of three differential equations for the temporal development of the fluid. This system describes the plasma in the so called single fluid. For the system to be complete it has to be supplemented by an equation of state, which describes the relation between pressure and density in the plasma. As already mentioned, the one-component description is only valid as long as no charge separation occurs over the length scales of concern. However, in some cases the plasma has to be modeled as a two – component system, taking care of the electrons and ions separately. This means the complete plasma description requires six instead of three equations, with the added complication of considering the interaction between the electron and ions via the Maxwell equations. Such an extended set of magneto-hydrodynamic equations can be quite complex. Again, analytical solutions of these equation systems exist for a very limited number of simple cases, so complex computer codes are normally needed to solve this set of equations (Piel, 2010).

## **1.12 Plasma Waves**

There are a large number of possible oscillations in system of coupled oscillators with as many degrees of freedom as plasma, and wavelike disturbance, e.g., electric fields  $E = E_0 \exp [i(K \cdot x - \omega t)]$ , will propagate in plasma. The frequency ( $\omega$ ) and the wave number  $K$  are functionally related to one another by a dispersion relation obtained from the plasma equations. Acknowledge of the dispersion characteristics ( $k$ )



for the propagating waves are certainly necessary for an understanding of the plasma state. The phase velocity of a wave is  $v_p = \omega/k$ , and the group velocity of a wave is  $v_g = \partial\omega/\partial k$ . Plasma can propagate both linear and nonlinear wave. The propagation of small amplitude waves is described by linearized equations. For examples (ion-sound waves and electromagnetic waves) (Krall and W, 1973). And the large amplitude waves is described by nonlinear. For example shock waves, parametric instabilities include (stimulated Brillouin scattering, stimulated Raman scattering, decay instability, two-Plasmon instability, stimulated Compton scattering) (Eliezer, 2002).

In cold plasma, these latter waves become a simple oscillation at the plasma frequency, below which the electromagnetic waves do not propagate.

In a thermal plasma, however, there are sound-like waves near this frequency, and in a plasma with disparate electron and ion temperatures with  $T_e \gg T_i$ , there is even a kind of hybrid sound wave that depends on the electron temperature and the ion mass. These waves even damp through a non-dissipative process. While these several kinds of behavior are already much more complicated than waves in ordinary fluids, they are very simple compared to the complexities added by a magnetic field. Even the kinds of nonlinearities in this simple plasma are richer in both diversity and complexity than in fluid dynamics where only averages over the velocity distribution are analyzed (Swanson, 2003).

The plasma properties can be discussed in two different categories:

### **1.12.1 Unmagnetized Plasmas**

Unmagnetized plasmas are generally the first to be studied because they are isotropic, i.e. the properties are the same in all directions. The

waves that such a plasma will support are either high frequency electromagnetic waves which see the plasma as a simple dielectric due to the response of the electrons to the wave (by comparison the ions are generally immobile), or sound-type waves (Swanson, 2003).

### **1.12.2 Magnetized Plasmas**

The addition of magnetic field effects to the subject of plasma waves adds a host of new phenomena, among which are: anisotropy, since there is now a preferred direction; new kinds of transverse waves existing only in magnetized plasmas, which we call Alfvén waves; finite Larmor orbit effects due to thermal motions about the magnetic field lines; and many other kinds of waves which are either totally new or greatly modified. Because of the anisotropy, the description of these effects is inevitably complicated algebraically, and this tends sometimes to obscure the physics. We shall, however, try to give the general descriptions, which are formidable, and show enough special cases to illustrate the richness of wave phenomena which are found in magnetized plasma. Even in cold plasma where thermal effects are absent, the number of wave types added by the inclusion of the magnetic field is large, and wave types vary greatly with the angle of propagation with respect to the magnetic field. We find waves which are guided by the magnetic field in certain frequency ranges, and cases where the phase and group velocities are nearly normal to one another. Whereas in cold unmagnetized plasma, the only parameter that may lead to inhomogeneities is the plasma density, the magnetic field not only adds a possible new source of inhomogeneity, but the gradients may appear in different directions. Since nearly all of the realistic plasmas, both in the laboratory and in ionospheric and

astrophysical plasmas, have a magnetic field, we shall expend considerable effort studying these effects and attempt to sort out the somewhat bewildering array of phenomena (Swanson, 2003).

### **1.12.3 Thermal Plasmas**

When thermal effects are added to the cold plasma effects, the new phenomena can be grouped into two general categories: acoustic wave phenomena due to various kinds of sound waves; and kinetic phenomena due to the fact that in a thermal or near thermal distribution, there are some particles moving at or near the phase velocity. These particles have resonant interactions with the waves due to their long interaction time with the wave. These interactions can lead to either collisionless wave damping or to instabilities and wave growth. When coupled with magnetic field effects, finite Larmor orbit effects lead to even more new wave types and instabilities (Swanson, 2003).

### **1.12.4 Landau Damping**

Landau damping is a characteristic of collisionless plasmas, but it may also have application in other fields. For instance, in the kinetic treatment of galaxy formation, stars can be considered as atoms of plasma interacting via gravitational rather than electromagnetic forces. Instabilities of the gas of stars can cause spiral arms to form, but this process is limited by Landau damping. There are actually two kinds of Landau damping: linear Landau damping, and nonlinear Landau damping. Both kinds are independent of dissipative collisional mechanisms. If a particle is caught in the potential well of a wave, the phenomenon is called "trapping." As in the case of the surfer, particles can indeed gain or lose energy in trapping (Chen, 1984).

### **1.12.5 Pondermotive Forces**

Light waves exert a radiation pressure which is usually very weak and hard to detect. Even the esoteric example of comet tails, formed by the pressure of sunlight, is tainted by the added effect of particles streaming from the sun. When high-powered microwaves or laser beams are used to heat or confine plasmas, however, the radiation pressure can reach severalhundred thousand atmospheres! When applied to plasma, this force is coupled to the particles in a somewhat subtle way and is called the pondermotive force. Many nonlinear phenomena have a simple explanation in terms of the pondermotive force. (Chen, 1984).

### **1.13 Shock Waves**

A shock wave is created in a medium that suffers a sudden impact (e.g. a collision between an accelerated foil and a target) or in a medium that Releases large amounts of energy in a short period of time (e.g. high explosives). (Eliezer,2002)Shockwaves are propagating hydrodynamic disturbances characterized by very steep density and pressure gradients at their leading edge. A shock wave develops in a medium when a disturbance such a piston motion travels through it supersonically(Burdiak,2014).When a pulsed high-power laser interacts with matter, very hot plasma is created. This plasma exerts a high pressure on the surrounding material, leading to the formation of an intense shock wave, moving into the interior of the target. The momentum of the out-flowing plasma balances the momentum imparted to the compressed medium behind the shock front. The thermal pressure together with the momentum of the ablated material drives the shock wave (Eliezer, 2002).As a consequenceof Newton's third law of dynamics (principle of action and reaction), the rest of the material is pushed inside creating a shock wave which compresses the material. This allows very high pressures

to be obtained (Megabar range). However, usually, laser produced shocks have a “poor” quality, a fact which has long prevented their use as a quantitative tool in high pressure physics. Shock wave EOS experiments are based on the use of Rankine- Hugoniot equations which, in the limits of very strong shocks, are:

$$\rho(D - u) = \rho_0 D \quad (1.26)$$

$$P - P_0 = \rho_0 D u \quad (1.27)$$

$$E - E_0 = u^2/2 \quad (1.28)$$

and respectively represents the conservation of mass, momentum and energy across the shock front. In these equations  $\rho$  is the density,  $D$  the shock velocity,  $u$  the fluid velocity in the compressed material,  $P$  the pressure and  $E$  the internal energy (Batani et al., 2003).

### 1.13.1 Scaling of Shock Pressure with Laser Intensity

In recent years, laser driven shock waves have begun to be a usable tool in high pressure physics, in particular in experiments for the determination of Equation of State (EOS) of materials at Mega bar pressures. There are a few kinds of pressure in laser produced plasma.

I. First Kind: The light pressure  $P_L$  in laser produced plasma caused by the direct laser radiation:

$$P_L = \frac{I_L}{C} (1 + R) \approx 3.3 \text{ Mbar} \left( \frac{I_L}{\frac{10^{16} \text{ W}}{\text{cm}^2}} \right) (1 + R) \quad (1.29)$$

Where  $R$  is the laser reflectivity ( $0 < R < 1$ ),  $I_L$  is the incident laser intensity and  $C$  is the speed of light. So for very high laser irradiance, the radiation pressure will be an extremely high one of the

effects of  $P_L$  is to steepen the density gradient near the critical density (Eliezer,2002).

II. Second Kind : The pressure in laser produced plasma.in corona is the thermal pressure of plasma particles: the ‘cold’ electron pressure  $P_e$ ,the ‘hot’ electron pressure  $P_H$  and the ion pressure  $P_i$ , associated with the different temperatures  $T_e$ , $T_H$ ,and  $T_i$  accordingly ,the two electron temperatures are obtained if the electrons in the corona have two distinct velocity distributions.To a good approximation,the ideal gas equation of state may use, namely:

$$P_e = n_e K_B T_e \approx 1.6 \text{Mbar} \left( \frac{n_e}{10^{21} \text{cm}^{-3}} \right) \left( \frac{T_e}{\text{Kev}} \right) \quad (1.30)$$

$$P_H = n_H K_B T_H \quad (1.31)$$

$$P_i = n_i K_B T_i \quad (1.32)$$

II. Third Kind: The pressure in the critical layer in this equation the laser light is absorbed at the plasma critical layer:

$$P(\text{Mbar}) = 8.6(1/10^{14})^{2/3} \lambda^{-2/3} (A_t/2Z)^{1/3} \quad (1.33)$$

where  $I$  is the laser intensity on target in  $\text{W/cm}^2$ ,  $\lambda$  is the laser wavelength in  $\mu\text{m}$ , and  $A_t$  and  $Z$  are the mass number and the atomic number of the target (John, 1995).

III. Third Kind: In reality, the mass ablation rate scaling should also include time dependence. Indeed the plasma corona size becomes larger during the interaction, and the distance between the absorption region and the ablation surface ( $n_e$ ) solid material increases with time. This brings to a decoupling of the laser beam from the target and, as a result, the mass ablation rate decreases with time. In particular, it is found that the shock pressure is related to laser and target parameters by (Mora, 1982):

$$P(\text{Mbar}) = 11.6(I/10^{14})^{3/4}\lambda^{-1/4}(A/2Z)^{7/16}(Z^*t/3.5)^{-1/8} \quad (1.34)$$

Where the time  $t$  is in ns and  $Z^*$  is the average ionization degree in the plasma corona. Fig (1-12) explain the ablation pressure.

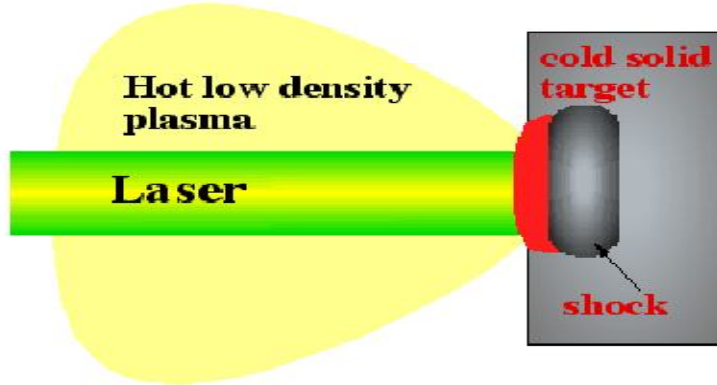


Fig (1-12): The ablation pressure

IV. Fourth Kind: In this formulawe get an equation, which is formally independent of time, but dependent on target thickness, i.e.

$$P(\text{Mbar}) = 15.63(I/10^{14})^{0.8}\lambda^{-4/15}(\rho_0)^{-1/15}d^{-2/15} \quad (1.35)$$

Where  $d$  is in  $\mu\text{m}$  (Batani et al 2006).

### 1.13.2 Shock Velocity

In the strong shock waves, the relation between shock velocity and shock pressure is equal:

$$D = \left( \frac{(\gamma + 1) P}{2 \rho_0} \right)^{1/2} \quad (1.36)$$

Where  $D$  is the shock velocity and  $\gamma$  is the adiabatic constant of the material and  $\rho_0$  is the unperturbed target density (Atzeni, 2004).

### 1.13.3 Coupling Parameter

The Coupling Parameters:

$$\Gamma_c = \frac{Z_c^2 e^2}{4\pi\epsilon_0 \langle d_m \rangle k_B T} \quad (1.37)$$

Is the ratio of the Coulomb interaction among two particles of species at the mean inter particle separation  $\langle d_m \rangle = (3/4\pi n_c)^{1/3}$  and the thermal energy  $k_B T$ . Plasmas characterized by  $\Gamma_c < 1$  are called weakly coupled. Their behaviour is largely governed by the temperature of the system. The individual particles can be considered as free particles, each moving independently of the others. Plasma observables are easily calculated by averaging the corresponding single-particle quantity over the Maxwell-Boltzmann distribution function. In the opposite case,  $\Gamma_c > 1$ , the term “strongly coupled plasma” is used. The mutual Coulomb interaction is larger than the mean kinetic energy of each particle. Hence, the calculation of observables is much more complicated, since the interaction of the particles has to be accounted for (Grades, 2008).

## 1.14 Plasma Industrial Applications

The unparalleled properties of the Fourth State of Matter such as high temperatures, energetic electrons and ions, and the existence of plasmas in a very wide range of densities, pressures, and temperatures often provide the only practical use in industry. Present plasma applications are discussed:

### 1.14.1 Semiconductor Electronics



The semiconductor electronics industry consists of the production of almost all of the high technology electronic devices such as computers, televisions, radios, cellular phones, etc. The typical semiconductor material is silicon found in the sand on the beaches. For this industry very large integrated circuits (chips) are produced. The widest use of plasma in industry today is the production of microelectronic devices (Elizer and Elizer, 2001).

#### **1.14.2 Plasma Spray**

Plasma spraying is used to apply a thick coating to substances that do not yield to other treatments. With the aid of plasma spraying an effective anti-corrosion coating is achieved, especially for high temperature industrial applications. Plasma spraying is done with a plasma gun, also called a plasma torch. This technique provides surface protection to turbine blades in aircraft engines, as well as many other tools and materials (Elizer and Elizer, 2001).

#### **1.14.3 Plasma Welding, Cutting and Material Processing**

Thermal plasma devices are widely used in welding and cutting hard materials. In welding, both the substrate and the filler metals are melted in order to achieve a strong metallurgical bond. In order for this method to be successful, both materials should have similar melting points. The welding process is also used for thick overlay (mm) coatings. For example, inclusions from the electrodes can cause porosity (full of pores). High pressure plasma in an equilibrium state between electrons and ions is used for basic material processing in industries such as melting, evaporation, and dissociation of minerals (such as oxides, carbides, and sulfides) (Elizer and Elizer, 2001).

#### **1.14.4 MHD Energy Conversion and Ion Propulsion**

Magnetohydrodynamic (MHD) energy conversion utilizes a dense plasma jet propelled across a magnetic field to generate electricity. The Lorentz force  $q\mathbf{v} \times \mathbf{B}$ , where  $v$  is the jet velocity, causes the ions to drift upward and the electrons downward,  $q$  is the charging the two electrodes to different potentials. Electrical current can then be drawn from the electrodes without the inefficiency of a heat cycle. The same principle in reverse has been used to develop engines for interplanetary missions (Chen, 1984).

### **1.14.5 Gas Lasers**

The most common method to "pump" a gas laser-that is, to invert the population in the states that give rise to light amplification-is to use a gas discharge. This can be a low-pressure glow discharge for a de laser or a high-pressure avalanche discharge in a pulsed laser. Some lasers used for alignment and surveying and the other lasers used in light shows.The powerfullaser used to cutting tool. Even solid state lasers, depend on a plasma for their operation, since the flash tubes used for pumping contain gas discharges(Elizer and Elizer, 2001).

### **1.15 Theoretical Models for Plasma**

The radiation emitted by the plasmas requires knowledge of both the charge state distribution and the excited level populations of different ions. This is possible by obtaining the solution of a complex system of rate equations, describing the population and depopulation of all the levels by the processes such as ionization, recombination, collisional excitation and de-excitation, radiative decay and absorption as well as the stimulated emission. Any given charge state is connected with its two neighboring states by the processes of ionization and recombination. Considering the difficulties associated in solving these

equations, the local thermodynamic equilibrium (LTE) and models suitable for ultra-high density, the approximations used in order of increasing electron density are: the corona model (CM) (Singh and Thakura, 2007). A plasma is said to be in a state of Complete Thermodynamic equilibrium (CT) if all of the following conditions are satisfied:

All particles obey the Maxwell velocity distribution law, the population distributions over the states of any atom or ion are given by the Boltzmann formula. The number of ions in a charge state  $z$  relative to the number in state  $(z-1)$  is given by the Saha equation. The intensity distribution of the radiation emitted can be described by the Planck radiation distribution function.

The 3 most common equilibrium models used to describe plasmas are:

- I. Local Thermodynamic Equilibrium
- II. Coronal Equilibrium
- III. Collisional Radiative Equilibrium

### **1.15.1 Local Thermodynamic Equilibrium**

Local Thermodynamic Equilibrium (LTE) is the name given to describe plasmas in which collisional excitation and de-excitation are the dominant atomic processes. Density must be high enough that an ion in an excited state has a greater chance of returning to the ground state through collisional de-excitation than through spontaneous emission. LTE is distinguished from complete thermodynamic equilibrium in that the temperature need not be the same everywhere, and the spectrum is not characteristic of a pure blackbody. Several conditions must hold true for LTE: The electron and ion velocity distributions should obey a Maxwell-Boltzmann distribution written as:

$$f(v)dv = 4\pi n_e v^2 \left\{ \frac{m_e}{2\pi k_B T_e} \right\} \exp \left\{ -\frac{m_e v^2}{2k_B T_e} \right\} dv \quad (1.38)$$

where  $f(v)$  is the density of the electrons with velocity between  $v$  and  $v + dv$ ,  $n_e$  is the electron density and  $T_e$  is the electron temperature.

The relationship between the electron density and temperature for LTE:

$$n_e \geq 1.6 \times 10^{12} T_e^{\frac{1}{2}} \chi(p, q)^3 \text{ cm}^{-3} \quad (1.39)$$

Where  $T_e$  is in Kelvin and  $\chi$  is the energy difference between levels  $p$  and  $q$  in electronvolts (Hoigh, 2010).

#### 1.14.2 Non-LTE Plasma

In plasma where the condition given above for LTE is not fulfilled, radiative processes are expected to play an important role in determining the population of the available energy states. In the general case all the possible electron processes will have to be taken into account and the populations of the levels will now depend upon atomic cross-sections. However, as these processes depend differently upon the electron density, one can expect that, in particular conditions, some of them will be more efficient than others, leading to a substantial simplification of the problem. If we assume that the plasma is optically thin, ion excitation and ionization will be supported by collisional processes. A question arises on how these processes are balanced, i.e. which of the possible de-excitation and recombination processes will have to be considered. In general, when the density is not high enough to ensure LTE, all inverse processes will contribute to de-excitation and recombination. On the other hand, if the density is sufficiently low, all collisional processes will become inefficient and only radiative de-excitation and recombination processes will have to

be considered. In this last case the problem can be simplified leading to the so called coronal model (Giulietti and Gizzi, 1998).

### **1.14.3 Coronal Equilibrium (CE)**

The coronal equilibrium is used to describe low density plasmas such as those found in nebulae or in the outer-regions of a star (the corona). At low densities (typically  $n_e < 10^{12} \text{cm}^{-3}$ ) the probability of radiative de-excitation transitions occurring now becomes comparable to (or even greater than) that of collisional de-excitation processes. The rate of collisional excitation is low in CE plasmas because the collision rates scale with electron density, meaning that electrons in excited states will have sufficient time in which to decay (radiatively) to their ground state before another collisional excitation event occurs. As a consequence most of the ions in the plasma are in their ground state. In CE plasmas, the mean free path of the photons is large and so the plasma is said to be optically thin. Because the radiation emitted within the volume of the plasma is not significantly re-absorbed as it travels through the plasma to the periphery region, photoexcitation and photoionization rates are negligible. Therefore one may assume that collisional processes (namely electron impact excitation and electron-impact ionization) excite the atoms/ions but rarely de-excite them, de-excitation being dominated by radiative processes (Dardis, 2009).

### **1.15.4 Collisional Radiative Equilibrium**

Collisional radiative equilibrium (CRE) is the name given to the model that describes an intermediate state between LTE and CE (typically  $n_e \approx 10^{19} - 10^{21} \text{cm}^{-3}$ ). Here both collisional and radiative processes have to be taken into account. The following conditions must be satisfied in order for CRE to hold: The velocity distribution

of the electrons must be Maxwellian to ensure that the Electron-electron relaxation time is smaller than the electron heating time.

The population density of ions of charge  $Z+1$  must not change significantly during the period when the quasisteady-state population distribution is being established among the ions of charge  $Z$ . The plasma must be optically thin to its own radiation(Hoigh,2010).

# **Chapter Two**

## **Plasma Temperature, Techniques of Measurements and Calculations**

### **2.1 Introduction**

The aim of this chapter is to explain the techniques, used for the determination of the electron temperature, in laser produced plasma.

### **2.2 Plasma Diagnostic Techniques**

For the characterization of plasmas, many diagnostic techniques are used including optical emission spectroscopy, laser induced fluorescence spectroscopy, mass spectroscopy, optical absorption spectroscopy, Langmuir probe method, interferometers, Thomson scattering, shadowgraphy, etc.

#### **2.2.1 Optical Emission Spectroscopy**

Optical Emission Spectroscopy (OES) is a very useful and versatile tool for analyzing laser produced plasmas. In particular OES can be used to extract temperatures and densities of plasmas (Hoigh, 2010).

#### **2.2.2 Laser Induced Fluorescence Spectroscopy**

Laser induced fluorescence (LIF) is the technique in which the laser frequency  $\nu$  is tuned to match a transition of a group of atoms or molecules, whose energy difference is  $E_{12}$ , by a relation  $\nu = E_{12}/h$ , and the resultant fluorescence is observed (Muraoka and Maeda 1993). The diagnosis of hydrogen atoms was a typical aim of the laser induced fluorescence (LIF) technique at the initial stage of its

applications to plasma experiments. LIF-technique used to the investigation of the plasma–surface interaction. Measurements of metal atom fluxes, the density of sputtered particles near plasma facing components, and the velocity distribution of sputtered atoms have been successfully investigated; for most metal atoms in the plasma boundary the LIF-technique can be applied if the density is higher than  $\sim 10^{12} \text{ m}^{-3}$  (Kikuchi et al., 2012).

### **2.2.3 Mass Spectroscopy**

The mass spectrometry has been used with multichannel deflection in time of flight (TOF) techniques and also in Fourier transforms spectrometers. Time of flight mass spectrometry (TOFMS) is very sensitive to the fast ions ejected from the laser irradiated surface. Ions with charge  $Ze$ , are collected using electric fields and then accelerated by a potential,  $V$ , down a field-free drift tube, each acquiring energy  $ZeV$ . The ions travel at different velocities  $v = (2ZeV/m)^{1/2}$  and arrive at a high gain detector such as multichannel plate (MCP) or channeltran, at different times, from which the mass-to-charge ratio ( $m/z$ ) is derived. The actual velocity with which the ions travel to the collection region is convoluted with the drift velocity (Harial, 1997).

### **2.2.4 Optical Absorption Spectroscopy**

The technique of optical absorption spectroscopy is used to analyzing the absorption of light which is radiated into plasma from the outside. Since the absorption is caused by species existing in the plasma, it is possible to identify species and to determine their densities. If the low particle density causes difficulty in obtaining sufficient signal strength, the light path that passes through the plasma may be made longer by utilization of multireflection with the help of mirrors. By using laser with narrow band as a radiation source, space and time



resolved spectra can be obtained at high sensitivity. The degree and rate of dissociation for a molecule can be determined by observing that specific species in the plasma (Geohegan and Puretzky, 1996).

### **2.2.5 Langmuir Probe**

The Langmuir or plasma probe is a practical instrument that has been widely used to investigate plasmas in the laboratory and in the space environment. This electrostatic device, first developed by Langmuir and Mott-Smith, gives a measure of the temperature and density of a plasma. A conducting probe, or electrode, is inserted into the plasma and the current that flows through it is measured for various potentials applied to the probe. When the surface of the probe is a plane, the current is measured as a function of potential. When the probe is placed in the plasma, the plasma reacts by shielding the probe potential, thus forming a sheath with thickness on the order of a Debye length (Inan and Gołkowski, 2011).

### **2.2.6 Interferometers**

Interferometers have been used as optical instruments for more than 100 years. Interferometers can be used to directly measure distance, displacement and vibration, and from these quantities density, temperature, refractive index and electron density can be inferred. They can also be used as spectroscopic elements. The three main types of interferometers, Michelson interferometer, Mach-Zender interferometer, Fabry-Perot interferometers (Muraoka and Maeda, 2001).

### **2.2.7 Thomson Scattering**

Thomson scattering (TS) has been a widely applied technique to investigate the electron component of thermonuclear plasma since the

first TS diagnostics was carried out in early 1963. TS refer to the scattering of electromagnetic waves by free electrons. It is based on Doppler broadening of the scattering spectrum, reflecting the velocity distribution of the electrons. The main characteristics that dominate the accuracy in most Thomson scattering (TS) diagnostics are the power of the probing source, the quantum efficiency of the detectors and the transparency of the collection optics with spectral devices. Lasers have a high spectral brightness and their beams can be focused in the plasma to produce a good spatial resolution. Also, lasers do not perturb the plasma owing to the relatively small interaction cross-sections (Mitsuru et al., 2012).

### **2.2.8 Shadowgraphy**

Shadowgraphy in its simplest form is the detection of variations in the transmitted intensity of a collimated light beam after it has passed through a (usually) non-uniform medium, for example, a laser produced plasma (Hoigh, 2010). Shadowgraphy used to determine the refractive index of plasma and the position of the shock wave. By the Refraction of light at the density gradients (Muraoka and Maeda, 2001).

## **2.3 Temperature and Equilibrium**

Maxwell's distribution for velocities of particles of mass 'M' gives the number of particles dN with velocity between v and v+dv in terms of their number density N and temperature T as follows:

$$dN(v) = N(M/2\pi kT)^{3/2} \exp(-mv^2/2kT) 4\pi v^2 dv \quad (2.1)$$

The Boltzmann distribution of particles  $N_j$  having excitation energy  $E_j$  is:

$$N_j = N[g_j/U(T)]\exp(-E_j/kT) \quad (2.2)$$

Where  $U(T) = \sum g_j \exp(-E_j/kT)$  is called the state sum or partition function.

The equilibrium distributions for kinetic energy, excitation energy and ionization energy are represented by Maxwell, Boltzmann and Saha equations respectively and it may happen that there is equilibrium distribution of one of these forms of energy but not for the others (Singh and Thakur, 2007). Under the equilibrium conditions of the Maxwell–Boltzmann distribution it is also possible to estimate the degree of ionization of a gas at a given average temperature. The ionization of individual atoms and molecules typically requires thermal energies of greater than 20 000 K. However, when a gas is in thermal equilibrium a considerable degree of ionization still occurs, even if the mean temperature of the gas is far below the ionization energy. This is because even a low-temperature gas at equilibrium contains a small but finite number of particles with very high velocities, in the “tail” of the Maxwellian distribution. The degree of ionization is determined by the balance between ionization by collision with high-energy particles and recombination. The exact solution of the problem, which takes into account quantum mechanical aspects, is known as the Saha equation:

$$\frac{N_i}{N_n} = 2.405 \times 10^{21} \frac{T^{3/2}}{N_i} \exp\left(-U/k_B T\right) \quad (2.3)$$

where  $N_i$  is the density of ionized atoms,  $N_n$  is the density of neutrals, and  $U$  is the ionization energy. The action of recombination is manifested in the presence of  $N_i$  in the denominator on the right-hand side. An ion–electron pair quickly recombines when in close

proximity, and because of quasi-neutrality their densities can be approximated as being equal ( $N_e \sim N_i$ ). Thus the higher the density of ions, the smaller the equilibrium degree of ionization, making it much easier to sustain a plasma state in gases at low densities (Inan and Gołkowski, 2011).

## **2.4 Measurement Techniques of Temperature**

There are a large number of methods that determine plasma properties by measurement of electromagnetic waves emitted by various species in the plasma. Measurement techniques based on wavelengths in the visible or near visible part of the spectrum have been developed since the beginning of this century, and are powerful techniques for the study of plasmas. In relatively low temperature plasmas, with temperatures of less than a few tens of thousands of degrees, many methods have been applied to different plasmas, and the techniques are well understood and well established. High-temperature plasmas that have temperatures of a few tens of thousands to a hundred million degrees have been developed for the goal of controlled thermonuclear fusion. In these high-temperature plasmas, many-electron atoms are multiple-ionized, and emission from these species, together with Bremsstrahlung from electrons, forms the bulk of the emitted radiation, at wavelengths ranging from the vacuum ultraviolet to the x-ray part of the spectrum (Muraoka and Maeda, 2001).

### **2.4.1 The Boltzmann Plot Technique**

For estimating the electron temperature of the plasma, the Boltzmann plot technique is among the most commonly used. This method utilizes the ratios of different line intensities of the same species to estimate the excitation temperature of the plasma. The intensities of

These lines are modified by certain parameters and then plotted against upper-level energy of the transition. If the fit is linear, then the assumption of a Maxwellian velocity distribution of the electrons is validated (Campos,2010).

$$n_{nm} = n_n \frac{g_m}{Z} e^{-E_m/KT} \quad (2.4)$$

Where  $n_{nm}$  is the population of the  $m$ -th excited state,  $n_n$  is the population of the ground state,  $g_m$  is the statistical weight of the upper level,  $Z$  is the atomic number,  $E_m$  is the upper level energy, and  $kT$  is the excitation temperature. The population of the energy state clearly affects the emission strength of that particular line's emission, and they can be related to by the following equation

$$I_{nm} \approx A_{nm} n_n \frac{g_m hc}{Z \lambda_{nm}} e^{-E_m/KT} \quad (2.5)$$

$I_{nm}$  is the intensity of the line, and  $A_{nm}$  is the lifetime of the upper-level of the transition. Because the plasma is assumed to be in LTE, estimating the temperature is a simple matter of moving the constants to the LHS of the equation and taking the natural log of each side. This gives the equation of a straight line with slope  $-kT$ , and because the quantity of interest is the slope,  $-kT$ , the constants ( $n_n$ ,  $h$ ,  $c$ , and  $Z$ ) can be ignored for calculation, so the equation to fit becomes

$$E_m = -\ln \left[ \frac{I_{nm} \lambda_{nm}}{g_m A_{nm}} \right] \times kT \quad (2.6)$$

Where the quantity " $I_{nm} \lambda_{nm} / g_m A_{nm}$ ," serves as  $x$  and " $kT$ " serves as  $m$  in " $y = mx$ " (Campos, 2010).

The temperature in terms of relative intensities of lines from the same

element and same state of ionization is given by:

$$kT = (E_2 - E_1) / \log_e(I_1 \lambda_1^3 g_2 f_2 / I_2 \lambda_2^3 g_1 f_1) \quad (2.7)$$

where  $I_1$  is the total intensity integrated over the line profile,  $\lambda_1$  is the wavelength and  $f_1$  the oscillator strength of the spectral line with excitation energy  $E_1$  and  $I_2, \lambda_2$  and  $f_2$  are the corresponding quantities for the line with excitation energy  $E_2$ , The statistical weights for energy states  $E_1$  and  $E_2$  are  $g_1$  and  $g_2$  respectively (Campos, 2010).

#### 2.4.2 Temperature from Doppler Profile

The most reliable spectroscopic technique of measuring kinetic temperature of atoms and ions is based on the measurement of the widths of Doppler broadened spectral lines. In the case of Maxwellian velocity distributions of emitting species such lines have Gaussian profiles with FWHM given by eq:

$$I(\nu) = I_0 (\gamma/4\pi)^2 / [(\nu - \nu_0)^2 + (\gamma/4\pi)^2] \quad (2.8)$$

Where  $I_\nu$  is the intensity at the center of the line profile  $\nu_0$  and  $\gamma$  is the radiation damping constant:

$$\gamma = (2\pi e^2 \nu^2) / (3\epsilon_0 m c^3) \quad (2.9)$$

Where  $m$  is the electron mass. The lifetime of a classical oscillator is the inverse of damping constant ( $\tau = 1/\gamma$ ) and it is of the order of  $10^{-8}$  sec for emission in the visible region. This spread of intensity over a range of frequencies is called natural broadening of the spectral line

and  $(\gamma/2\pi)$  is called full width at half maximum (FWHM). One must

make sure that the thermal Doppler Effect is the major cause of line broadening in the source before using this method of temperature measurement. It has been found that even gross motions in the source could simulate a Gaussian profile (Singhand Thakur, 2007).

### 2.4.3 Temperature from Shock waves

The temperature in the case of shock related to the shock velocity and given by:

$$T = \frac{D^2 m_i}{5K_B(\xi - 1)} \quad (2.10)$$

Where D is the shock velocity, and  $m_i$  is the atomic mass,  $K_B$  is the Boltzman constant,  $\xi$  is a number of electron in the outer shell (Osman, 2011).

Other equation used to calculate plasma temperature of shock wave depends on the intensity and wavelength of laser.

$$T_e(\text{eV}) = 10^{-6} (I(\text{w/cm}^2) \lambda^2 (\mu\text{m}))^{2/3} \quad (2.11)$$

Also we can write this equation by high pressure from eq(1.33)

$$I = \left( \frac{P}{(8.6 \times (\lambda^{-2/3}) * (A/2Z)^{1/3})^{2/3}} \right) \times 10^{14} \quad (2.12)$$

$$T_e(\text{eV}) = 10^{-6} * (I * \lambda^2)^{2/3} \quad (2.13)$$

This equation is used to calculate the plasma temperature of shock waves in Prague Asterix Laser System (PALS) laser experiments (Batani and Baton, 2011).

## 2.5 Literature Review

Dhareshwar, et al in 1992 studied the case of using Nd: glass laser focused to produce intensities in the range of  $10^{12}$ - $10^{14}$  W/cm<sup>2</sup> on the target, within an irradiation spot diameter of 160  $\mu$ m. Optical shadowgrams were recorded by a second harmonic (0.53  $\mu$ m wavelength) pulse. Shock pressures and scaling of pressure with laser intensity was studied. Shock pressures in gold-coated Plexiglas target was considerably higher compared to those in uncoated targets. This enhancement of shock pressure has been explained on the basis of contribution of an X-ray driven ablative heat wave in the gold plasma. Shock pressure values show a close agreement with those obtained from one-dimensional Lagrangian hydrodynamic simulation. Shadowgrams of shock fronts produced by non-uniform spatial laser beam irradiation profiles have shown complete smoothing when a gold layer is used on a Plexiglas target.

In 1996 Benuzzi et al reported that the High quality shock waves with direct- and indirect-laser drive were generated. They used the phase zone plate smoothing technique in the case of direct drive and thermal x rays from laser heated cavities in the case of indirect drive. The possibility of producing homogeneous, steady shock waves without significant preheating effects with both methods has been proved. By using such shocks, copper equation of state measurements have been performed up to 40 Mbar, which was previously obtained only with nuclear explosion in 1996. Experiment investigation of Laser-driven shock wave propagation in a transparent material such as Plexiglas coated with a thin over layer of gold was studied using the technique of high speed optical shadowgraphy.



A proposed experiment for the absolute measurement of the Equation of State (EOS) of solid materials in the 10–50 Mbar pressure range was analyzed by means of numerical simulations. In the experiment, an intense laser pulse drives a shock wave in a solid target. The shock velocity and the fluid velocity were measured simultaneously by rear side time-resolved imaging and by transverse X-radiography, respectively. An EOS point was then computed by using the Hugoniot equations. The target evolution was simulated by a two-dimensional radiation hydrodynamics code; (ad hoc) developed post-processors then generate simulated diagnostic images. The simulations evidence important two-dimensional effects, related to the finite size of the laser spot and to lateral plasma expansion. The first one may hinder detection of the fluid motion, the second results in a decrease of the shock velocity with time (for constant intensity laser pulses). A target design was proposed which allows for the accurate measurement of the fluid velocity; the variation of the shock velocity can be limited by the choice of a suitably time-shaped laser pulse. Reported by Temporal, et al in 1997.

In 2001 Zhanga et al. Reported a numerical study of the laser induced evaporation and ionization process during pulsed laser deposition is presented. The process is separated into three domains:

(i) Conduction inside the solid, (ii) a discontinuity layer between solid and vapor, and (iii) expansion of high temperature vapor plasma. A quasi-one-dimensional model was solved to predict the temperature field inside the solid. Mass, momentum, and energy are conserved across the discontinuity layer. Equations of mass, momentum, and

energy conservation are solved simultaneously to provide boundary conditions for the expansion process. Euler equations are used to model the expansion of high temperature vaporplasma. The Euler equations are integrated numerically using a Runge–Kutta scheme combined with flux vector splitting. The density, pressure, temperature, and velocity contours of the vapor phase are calculated and the results are analyzed.

In 2002 Pantet al presented Results of laser-driven shock wave experiments for equation-of-state (EOS) studies of gold metal. Nd: YAG laser chain (2 Joule, 1.06  $\mu\text{m}$  wavelength, 200 ps pulse FWHM) was used for generating shocks in the planar Al foils and Al + Au layered targets. EOS of gold in the pressure range of 9– 13 Mbar was obtained using impedance-matching technique. Numerical simulations performed using one dimensional radiation hydrodynamic code supports the experimental results. Experimental data show remarkable agreement with results from studies using the existing standard EOS models and with other experimental data obtained independently using laser-driven shock experiments.

Batani et al in 2003 was described the quality requirements that a shock wave must fulfil to make equation of state (EOS) measurements possible: planarity, no preheating and stationarity of the shock. Experimental measurements have been performed at the Max Planck Institut für Quantenoptik (Garching). They also presented simple analytical models that allow verifying shock stationarity and absence of preheating.

The GEKKO/HIPER-laser driven shock experiments were characterized in detail for studies of equation-of state (EOS) in ultra-

high pressure regime. High-quality shock waves were produced with optically smoothed laser beams. Key issues on EOS measurement with shock waves, the spatial uniformity and the temporal steadiness of shock, and the preheating problem were investigated by measurements of the self-emission and reflectivity from target rear surface. These experiments and analysis were based on impedance matching method validated by use of double-step targets consisting of two Hugoniot standard metals. Extreme shock waves previously only achieved in nuclear explosion experiments were generated using the laser direct-drive experimental scheme. This problem was discussed by Ozaki et al.,2004.

In order to study the hydrodynamics of laser produced plasmas, experiments were performed using the Prague PALS iodine laser working at 0.44  $\mu\text{m}$  wavelength and irradiances up to a few  $10^{14}\text{W}/\text{cm}^2$ . By adopting large focal spots and smoothed laser beams, the lateral energy transport and lateral expansion have been avoided. Therefore the workers could reach a quasi-one- dimensional regime for which experimental results can be more easily and properly compared to available analytical models. This problem was discussed by Batani et al2006.

In 2007 Batani et.al reported the generation of very-high pressures shocks by means of laser beams, and their use for Equation-of-State experiments on materials in the Megabar pressure ranges. In particular, they presented some applications to study EOS of carbon. Finally, they discussed non-equilibrium processes in laser-driven shocks.

Boustie et.al. In 2008 showed that the High power pulsed laser interaction with matter yields to very high amplitude pressure loadings

with very short durations, initiating into solids a strong short shock wave. Compared to the conventional generators of shock (launchers of projectiles, explosives), these particular characteristics offer the possibility to study the behaviour of matter under extreme dynamic conditions, with a possible recovery of the shocked samples presenting the effects of the passage of the shock in most cases. This work introduces the principle of laser shock generation, the characterization of these shocks, principal mechanisms and some effects associated with their propagation in the solids.

In 2011 Aliverdievet al used a series of numerical simulationsthat performed on the application of the impedance mismatch technique to the experimental study of the equation of state (EOS) of porous carbon. They concluded that this technique was useful for such a study up to laser intensities of the order of  $10^{14}$  W/cm<sup>2</sup> (in second or third harmonic of theNd-YAG laser). However, the inclusion of the radiation transport was important for the correct description of the shock propagation and can affect the results.

A theoretical study of equation of state (EOS) properties of fluid and dense plasma mixtures of xenon and deuterium was done by Magyar, et al in 2013, to explore and illustrate the basic physics of the mixing of a light element with a heavy element. Accurate EOS models are crucial to achieve high-fidelity hydrodynamics simulations of many high-energy-density phenomena, for example inertial confinement fusion and strong shock waves. While the EOS was often tabulated for separate species, the equation of state for arbitrary mixtures was generally not available, requiring properties of the mixture to be approximated by combining physical properties of the pure systems. Density functional theory (DFT) at elevated-temperature was used to

assess the thermodynamics of the xenon-deuterium mixture at different mass ratios. The DFT simulations were unbiased as to elemental species and therefore provide comparable accuracy when describing total energies, pressures, and other physical properties of mixtures as they do for pure systems. The study focuses on addressing the accuracy of different mixing rules in the temperature range 1000–40 000K for pressures between 100 and 600 GPa (1–6 Mbar), thus, including the challenging warm dense matter regime of the phase diagram. They found that a mix rule taking into account pressure equilibration between the two species performs very well over the investigated range.

In 2014 deRességuier, et.al. Reported that the high pressure shock compression induces a large temperature increase due to the dissipation within the shock front. Hence, a solid sample subjected to intense shock loading can melt, partially or fully, either on compression or upon release from the shocked state. In particular, such melting was expected to be associated with specific damage and fragmentation processes following shock propagation. In this work, they showed that laser driven shock experiments can provide a procedure to investigate high pressure melting of metals at high strain rates, which was an issue of key interest for various engineering applications as well as for geophysics.

In 2014 Saliket.al, presented that the spectroscopic studies of the plasma generated at the surface of manganese sulfate by the fundamental (1064 nm) and second harmonic (532 nm) of a Q-switched Nd:YAG laser. The  $4s4p\ ^4F_{7/2} \rightarrow 4s\ ^2H_{9/2}$  at 438.80 nm,  $4p\ ^2I_{11/2} \rightarrow 4s\ ^2I_{11/2}$  at 440.80 nm,  $4p\ ^4G_{11/2} \rightarrow 4s\ ^2H_{9/2}$  at 464.27 nm,  $4p\ ^4F_{5/2} \rightarrow 4s\ ^4D_{7/2}$  at 467.16,  $4p\ ^4F_{5/2} \rightarrow 4s\ ^4G_{7/2}$  at 515.08 nm, and  $4p$

${}^4F_{7/2} \rightarrow 4s^2 {}^4G_{9/2}$  at 519.65 nm transitions have been used to estimate the electron temperature through the Boltzmann plot method. The number density has been estimated from the Stark broadened profiles of the spectral line 348.30 nm. The spatial behaviour of the electron temperature and number density has been examined at different ambient air pressures and with laser irradiance. The temperature and number density are found to be in the range from 9842 K to 9371 K and  $1.58 \times 10^{17}$  to  $3.26 \times 10^{16} \text{ cm}^{-3}$  for the 1064 nm laser, from 9668 to 9297 K and  $2.27 \times 10^{17}$  to  $5.79 \times 10^{16} \text{ cm}^{-3}$  for the 532 nm laser.

# **Chapter Three**

## **The Computer Simulation**

### **3.1 Introduction**

The aim of this chapter is to present some detailed information about hydrodynamic Modeling that was the basis of the computer simulation used in this work to calculate the electron plasma temperature in the plasma produced in alkaline earth group elements using different lasers. The chapter presents the properties of the targets and the lasers, and the flow chart of the simulation.

### **3.2 Modeling Method**

Modeling is a tool for investigating the experiment before it is performed. It provides to check whether the input data are satisfactory or not, by means of this Prescience the experimental set-up together with time can be saved. Moreover, it helps to decide the experiment in detail and calculates some quantities that cannot be directly measured. Besides, data from the experiments can also be investigated (Y,2006).

### **3.3 Numerical Simulation**

Both in the kinetic and in the fluid description, the equations describing collisionless plasma in self-consistent electromagnetic fields are strongly nonlinear. Analytical solutions are hard to find and in a limited number. Thus, a crucial role is played by simulations, i.e. by the numerical solution of the model equations for given geometry and boundary conditions. The continuous increase in computing

power allows simulations to consider progressively larger system sizes and calculation times approaching those typical of experimental Observations. At the same time, relatively complex simulations may be already performed on cheap personal computers. For these reasons, a larger part of the laser-plasma community is now using simulation codes, some of the latter being freely available. Numerical simulations are essential tools of physics, particularly of plasma physics, and their importance and utility in the study of laser plasmas may hardly be overestimated. Still, it is important that the users do not always use a code written by someone else as a black box, but have some insight about what is inside the code, including a basic knowledge of algorithms and numerical methods. (Macchi, 2013).

### **3.4 Matlab Program**

Matlab is the software developed by the MathWorks, Inc., Natick, USA. In 1984, the first version appeared. Software was primarily used only for the mathematical computation enabling the computation of complicated matrix equations and their systems. All major functions can directly use the matrix as the input. Matlab became the standard in the area of simulation and modelling and it is used by the researchers and students at universities mainly in the areas of Control Engineering, Power Plant Systems, Aerospace, Bioinformatics, Economics and Statistics.

Graphical User Interface (GUI) is an environment available with renowned software that gives the option to the user developing software packages for personal and problem specific uses. It is a way of arranging information on a computer screen that is easy to understand and use because it uses icons, menus and a mouse rather than only text and programs written in high level language which is



often not much handy for others except for programmers(Leite , 2010). Matlab program was used to create and running the simulation in this work.

### 3.5 Target Materials

Alkaline earth group, or group (II) from periodic table were used as the targets in this work. The alkaline earth group include: (Beryllium (Be), Magnesium (Mg), Calcium (Ca), Strontium (Sr), Barium (Ba), Radium (Ra) .Table (3-1) lists the properties of the elements in this group.

Table(3-1):The properties of the Alkaline Earth group

Name	Symbol	Atomic number	Atomic mass	Density(g/cm <sup>3</sup> )
Beryllium	Be	4	9.012182	1.8477
Magnesium	Mg	12	24.305	1.738
Calcium	Ca	20	40.078	1.55
Strontium	Sr	38	87.62	2.54
Barium	Ba	56	137.327	3.51
Radium	Ra	88	226.0	5.0

### 3.6 Lasers Used in the Simulation

Many types of lasers were used in this simulation work:

#### 3.6.1 Nd-YAG Laser

Nd:YAG solid laser is widely used in laser produced plasma,due to the ultra-high peak power that can produced by the short pulse type of this laser. The fundamental wavelength of aNd:YAG laser(1064 nm) can be down-converted to shorter wavelengths (532, 354.7 and 266 nm) by means of passive harmonic generation techniques utilizing

nonlinear crystals (like e.g. KDP or BBO). Nd:YAG lasers are commercially available in a wide range of sizes and output powers (Musazzi and Perini, 2014).

### **3.6.2 Excimer Laser**

Excimer lasers are important because they are the only lasers capable of producing high-power in the ultraviolet (UV) region with good electrical efficiency. Commercially, the most important excimers are the rare-gas halide variety, such as krypton fluoride (KrF) with output at 248 nm, argon-fluoride (ArF) at 193 nm, and xenon chloride at 308 nm. There are other, less common excimer lasers based on transitions in xenon fluoride (XeF) at 353 nm, and in fluorine F<sub>2</sub>, which is not a rare-gas halide excimer but uses similar lasing mechanisms emitting at 157 nm (Hitz et al., 2001). Krypton fluoride (KrF) with output at 0.248  $\mu\text{m}$ , and argon-fluoride (ArF) at 0.193  $\mu\text{m}$  were used in the simulation work.

### **3.6.3 Iodine Gas Laser**

Iodine laser system was served also in this simulation both fundamental ( $\lambda = 1.315 \mu\text{m}$ ) and the third harmonic (0.438  $\mu\text{m}$ ) were used here. Fig (3-1) shows the iodine laser system. Used in the European program of laser produce plasma (Batani and Baton, 2011).



Fig (3-1) The Iodine laser system

### **3.7 The Simulation Work**

This simulation is based on the Equation of state to calculate the electron plasma temperature of shock waves. Equations (1.33), (1.36), and (2.13) were used to creating simulation program.

#### **3.7.1 Program Input**

The input parameters of the program consists of two parts, part one depend on the material parameters and part two depend on the laser parameters.

##### **3.7.1.1 Material Parameters**

The list of material parameters are: atomic number, atomic mass, initial density, this parameter fixed in the program and the thickness is interring manually.

##### **3.7.1.2 Laser Parameters**

The laser parameters that must be introduced in the program are: the intensity of the laser ( $\text{W/m}^2$ ), wavelength ( $\mu\text{m}$ ) and, pulse duration (ns).

### **3.7.2 Program Outputs**

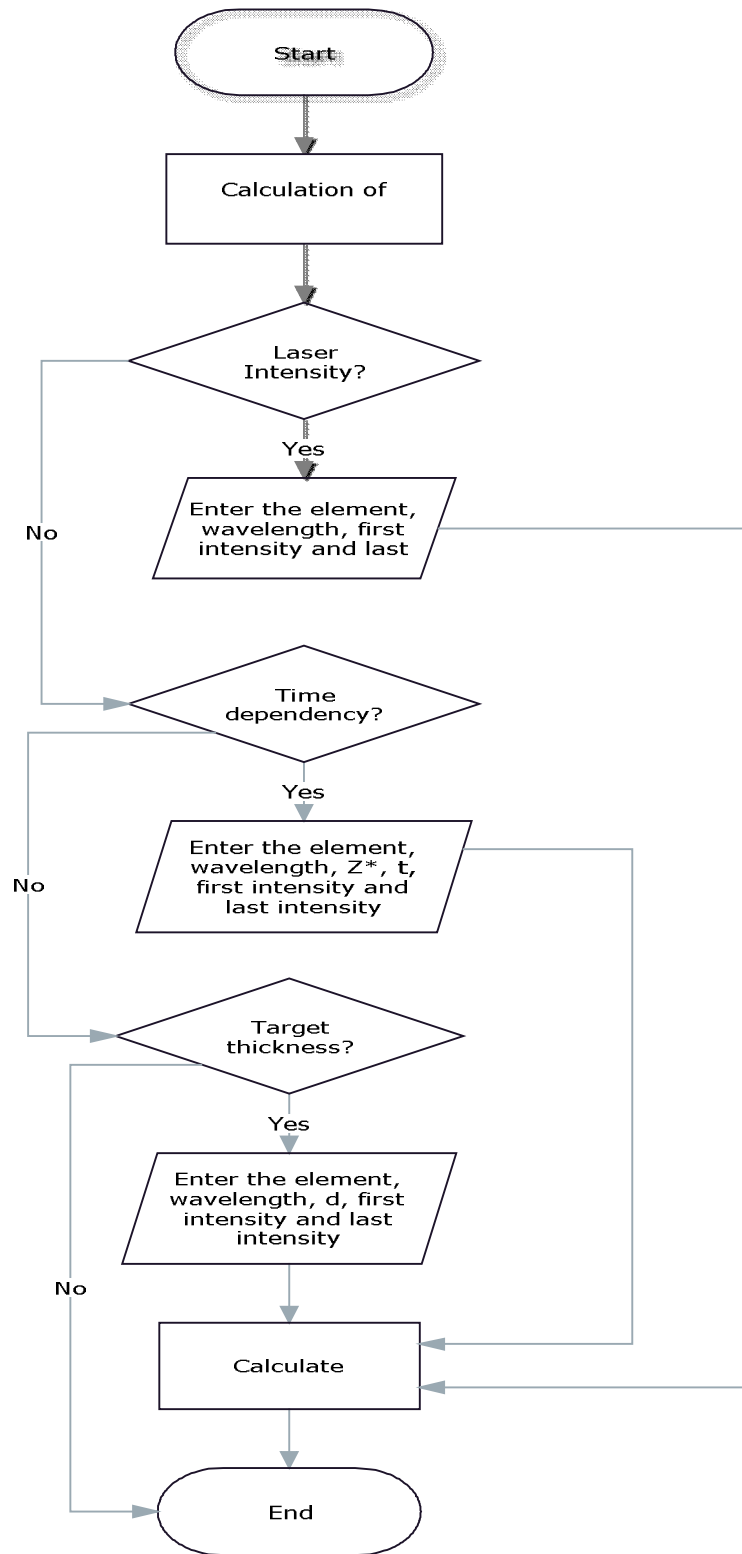
The outputs of the program governing the various plasma parameters such as high pressure of shock wave, shock velocity, and plasma electron temperature.

### **3.8 Program Structure**

Many Flow charts were used in this simulation .The first flow chart was used to calculate the electron plasma temperature and explain the relation between the electron temperature and laser intensities. The second flow chart was used to find the relation between the plasmaelectron temperature and laser wavelength. The third flow chart was used to explain the relation between the plasma electron temperature and the atomic numbers of materials.

#### **3.8.1 The Relation between the Plasma Electron Temperature and Intensities of Lasers:**

This part consists of three ways to calculate the plasma temperature electron, first way when the high pressure is generated in the critical layer eq (1.32). Second way related to the high pressure with pulse duration after that we inter the intensities of the laser, and wavelength, time, duration .The third way, related the high pressure with knowing thickness. In this program high pressure used in the critical layer. Beginning first with start and after that input the intensity, and wavelength and calculate the electron plasma temperature and to plot the relation between the electron plasma temperature with intensities. Figs (3-2) show the flow chart for this stage.



Fig(3-2):Flow chart of the relation between electron temperatures with laser intensities

### 3.8.2 Determination of the Relation between Plasma Electron Temperature and Wavelengths of the Lasers:

A flow chart was used to present the relation between plasma electron temperature and lasers wavelengths, first step is to input the intensities of all lasers, and after that the program calculate the pressure, shock velocity, electron temperature, finally plot the relation between electron plasma temperature and wavelengths, fig (3-3) show the flow chart of this stage.

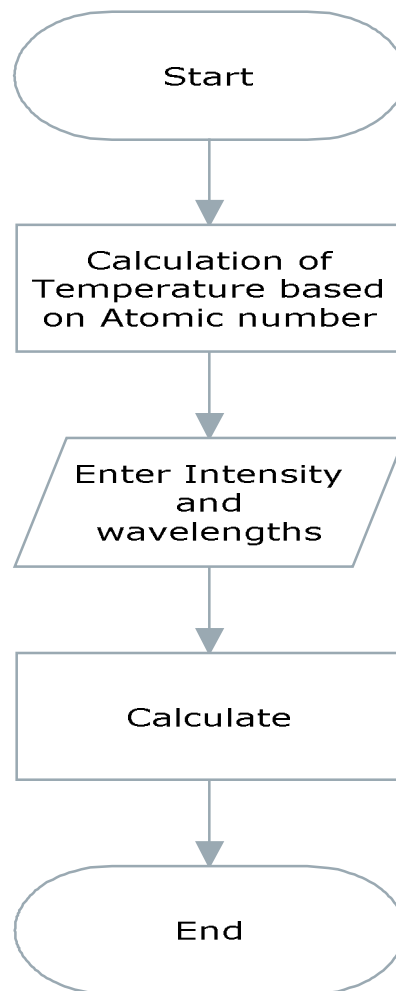


Fig (3-3): Flow chart of the relation between electron temperature and wavelength of lasers

### 3.8.1.3 The Relation between the Electron Temperature and Atomic Numbers of: the elements

This stage was used to determine the relation between the plasmaelectron temperature and atomic numbers of material, first step was input the wavelength of all lasers, and after that calculate the pressure, shock velocity, electron plasma temperature. Finally plot the relation between plasmaelectron temperature and atomic numbers of materials, fig (3-4) illustrates the flow chart of this stage.

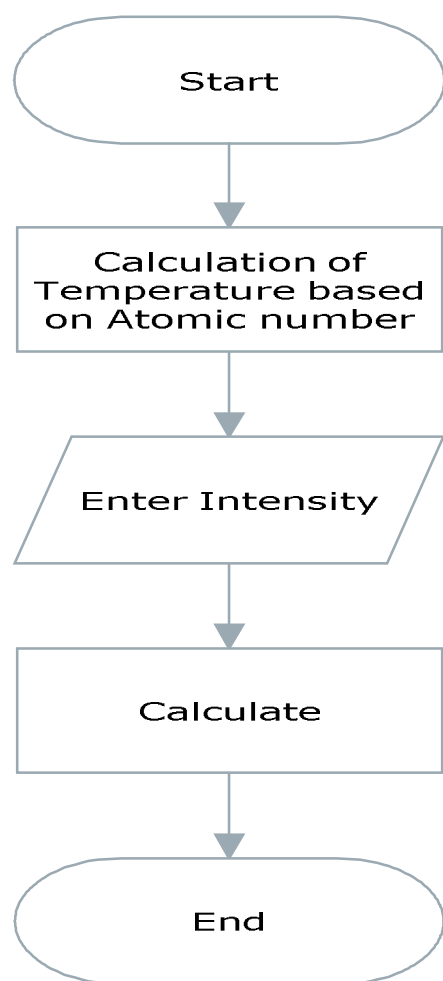


Fig (3-4): Flow chart of the relation between the electron plasma temperature and atomic numbers of materials

### 3.9 The Program Screens

The simulation program content several Screens, welcome screen is the first step of the program. Fig (3-5) shows this screen.

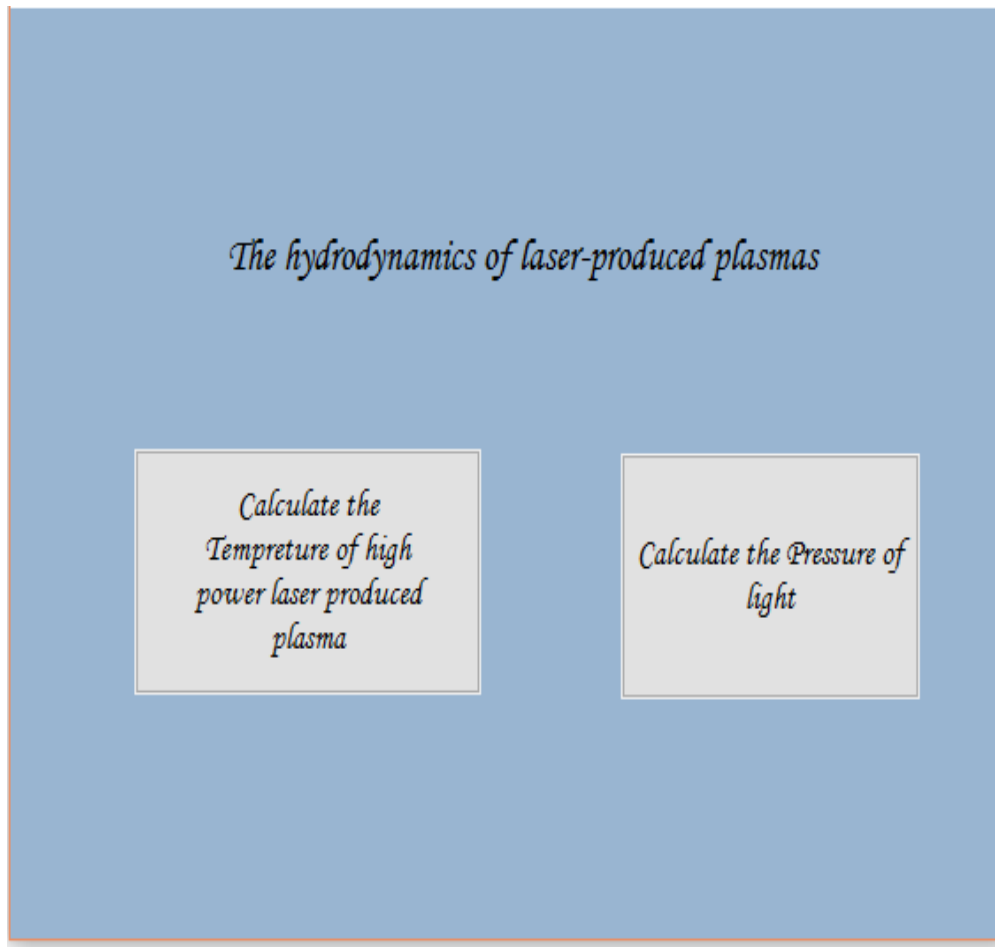


Fig (3-5): The two parts of the first screen

It consists two parts, part one to calculate the pressure of laser light fig (3-6) presented the detailed of this part. First input the range of intensity, laser reflectivity and steps were input and press next to view the results.



The image shows a software interface with a light blue background. It contains three input fields for data entry:

- The first field is labeled "Intensity(I):" and is followed by the word "from", a white input box, the word "to", another white input box, and the unit "(W/cm<sup>2</sup>)".
- The second field is labeled "# of steps:" followed by a white input box.
- The third field is labeled "Laser reflectivity(R):" followed by a white input box.

At the bottom of the interface, there are two buttons: "Cancel" on the left and "Next" on the right, both with a light gray background and a thin border.

Fig (3-6): The steps to calculate the pressure of the laser

Second part of the screen was used to calculate electron plasma temperature this part called the **Temperature of High Power Laser Produced Plasma (THPLPP)** see in fig (3-5)

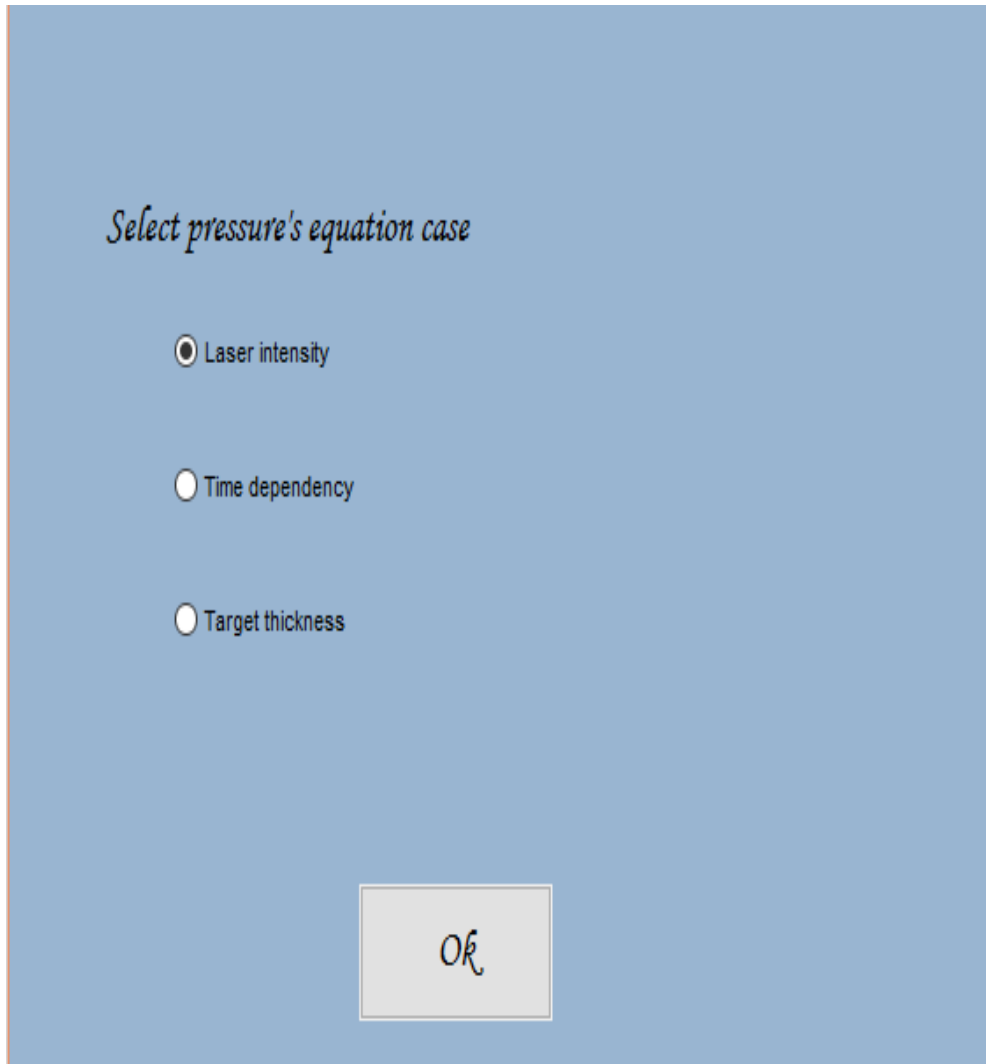


Fig (3-7): The screen explain the pressures equations

In this part we found several statuses of the pressure in plasma when, we press the (THPLPP) the choices of pressures was viewed, when we press the laser intensity, the other screen was opened and inter the parameters of laser were input fig (3-8) shows the details of the stage.

Select an element from the list below

Enter the following values

Element sample:  Mass number (A):  Number of electrons in the outer shell:

Atomic Number(Z):  Atomic mass(mi):  Initial Density( $\rho$ ):  ( $g/cm^3$ )

Degree of freedom of the system(N):  Wavelength( $\lambda$ ):  ( $\mu m$ )

Intensity(I): from  to  ( $W/cm^2$ ) # of steps:

Fig (3-8): The details of the pressure in the critical layer to calculate the electron temperature and plot the relation between electron temperature and intensities of the laser

The parameters of the material included in the simulation, when we chose the material, the parameters were viewed the selection from the list found in the program, when we finished, and press next, the result was viewed in the box and graph. If we use the equation of pressure included the time duration select the time depends from fig (3-9) explained that, then were press next , and the input of the equation of

pressure dependent of the time was viewed fig(3-5) explain that, and inter the parameter of laser and press next ,the result was obtained by box and graph.

Select an element from the list below

Enter the following values

Element sample:  Mass number (A):  Number of electrons in the outer shell:

Atomic Number(Z):  Atomic mass(mi):  Initial Density(ρ):  (g/cm<sup>3</sup>)

Average ionation degree (Z<sup>+</sup>):

Degree of freedom of the system(N):  Time (t):  Wavelength(λ):  (μm)

Intensity(I): from  to  (W/cm<sup>2</sup>) # of steps:

Cancel Next

Fig (3-9): The high pressure with time duration to calculate the electron temperature and plot the relation between electron temperature and intensities of the laser

To solve the equation of pressure by the thickness of target select the thickness from fig (3-10) shows the detail this is stage.

Select an element from the list below

Enter the following values

Element sample:  Mass number (A):  Number of electrons in the outer shell:

Atomic Number(Z):  Atomic mass(m):  Initial Density( $\rho$ ):  (g/cm<sup>3</sup>)

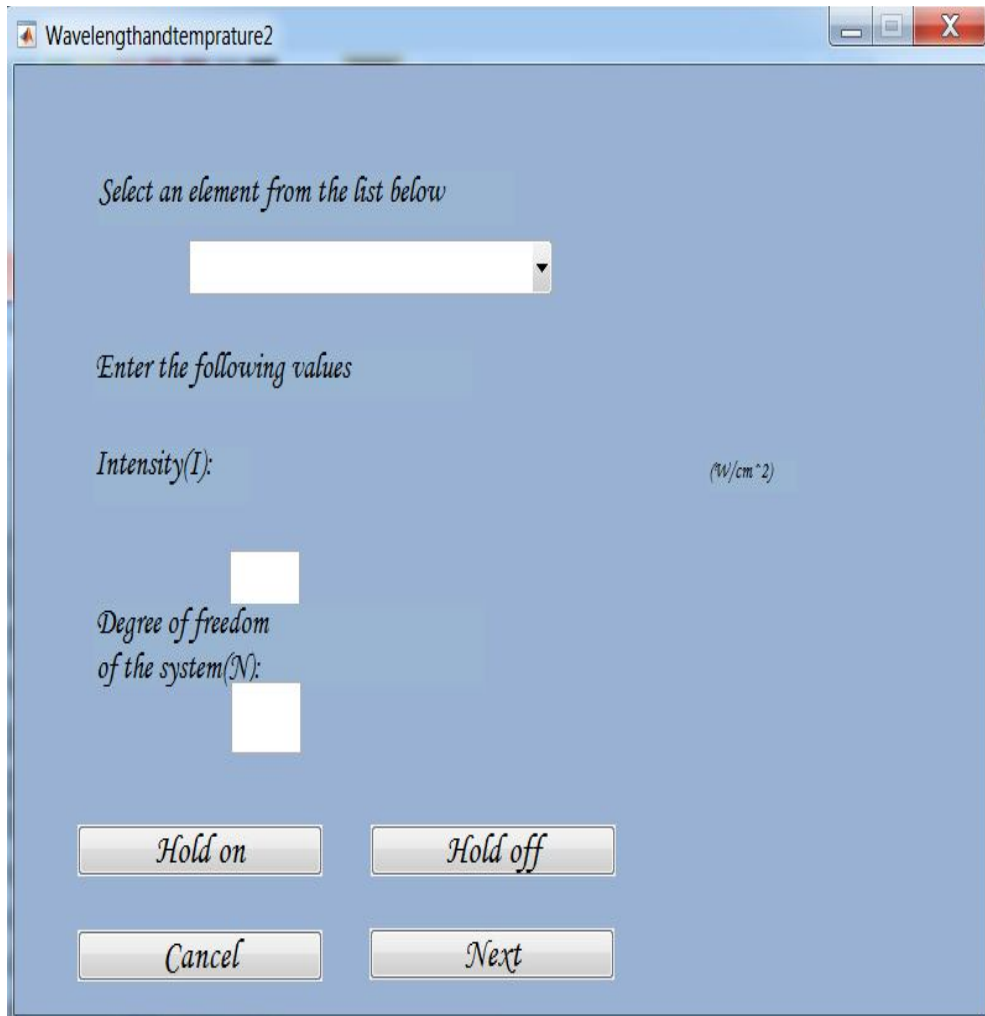
Degree of freedom of the system(N):  Wavelength( $\lambda$ ):  (μm) Target thickness (d):  (μm)

Intensity(I): from  to  (W/cm<sup>2</sup>) # of steps:

Fig (3-10): The screen used to calculate the electron temperature and plot the relation between electron temperature and intensities of the laser

and press next, the screen of this equation was viewed and inter the parameter of laser and the thickness of target and the parameter of material was also included in the program , enter all input and press next, the result was seen in box and graph.

Fig(3-11) shows the details of this stage. First we select the material, and after that inter the intensities and degree of freedom and press hold on and inter again the second intensity, and press hold on until inter all intensities, and after that we press hold off and next the plot between electron plasma temperature and wavelength of lasers will a pair.



Fig(3-11):The relation between the electron temperature and wavelength of lasers

Fig (3-12) shows the screen of this stage. First step is to plot this relation inters the intensity and wavelength, degree of freedom, and press hold on-again inter the second wavelength, and hold on, if we inter all wavelength press hold on and hold off and next, the graph of the relation is viewed.

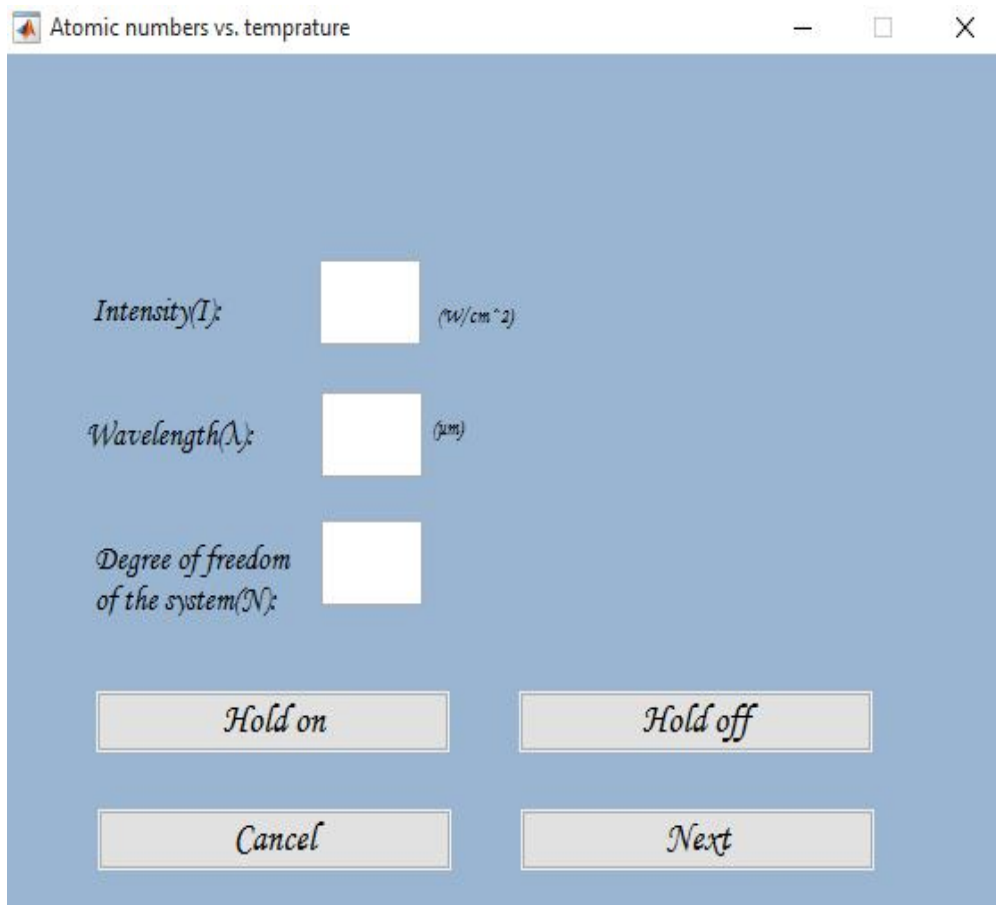


Fig (3-12): The steps to find the relation between electron temperature and atomic numbers of elements

# Chapter Four

## Results and Discussion

### 4.1 Introduction

In this chapter, the results are presented and after that they are discussed. In this simulation several types of lasers were used with different power densities. With different intensities as listed in table (4-1) below.

The aim of simulation is to calculate the electron temperature of the plasma produced from Alkaline earth Group (Be, Mg, Ca, Sr, Ba, Ra) used as targets. Matlab program was used to created and running the simulation. Additionally some conclusions and suggestions for future work are presented at the end of the chapter.

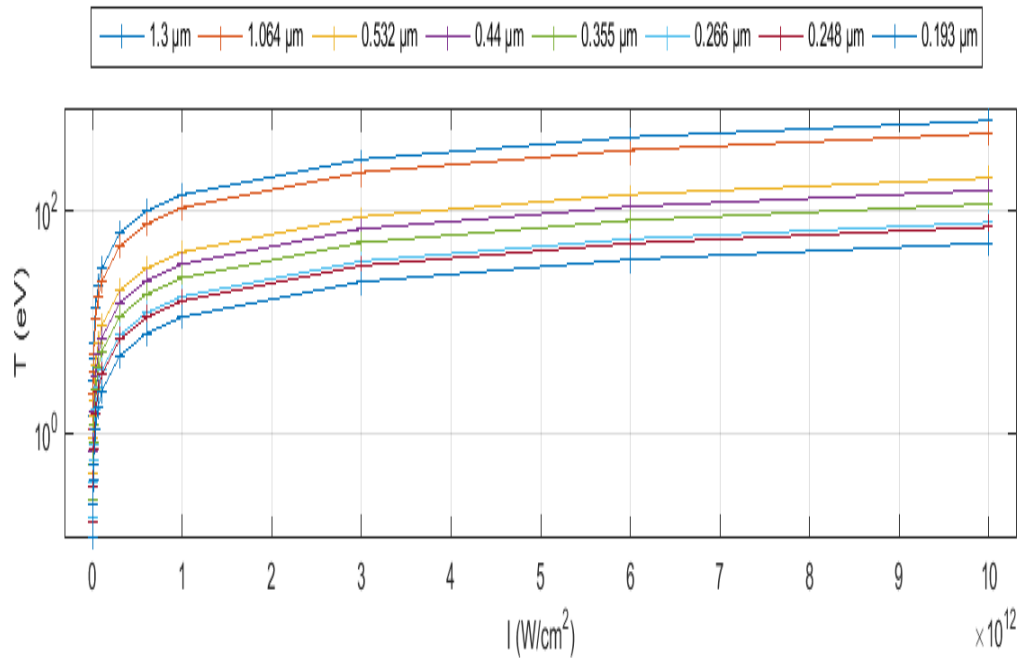
Table (4-1): The parameters of lasers used in the simulation

Lasers	Wavelength( $\mu\text{m}$ )	I( $\text{W}/\text{cm}^2$ )
Iodine laser	1.3	$1 \times 10^9$
	0.44	$3 \times 10^9$
Nd-YAG laser	1.064	$6 \times 10^9$
	0.532	$1 \times 10^{10}$
	0.355	$3 \times 10^{10}$
KF laser	0.248	$6 \times 10^{10}$
AF laser	0.193	$1 \times 10^{11}$
		$3 \times 10^{11}$
		$6 \times 10^{11}$
		$1 \times 10^{12}$
		$3 \times 10^{12}$
		$6 \times 10^{12}$
		$1 \times 10^{13}$

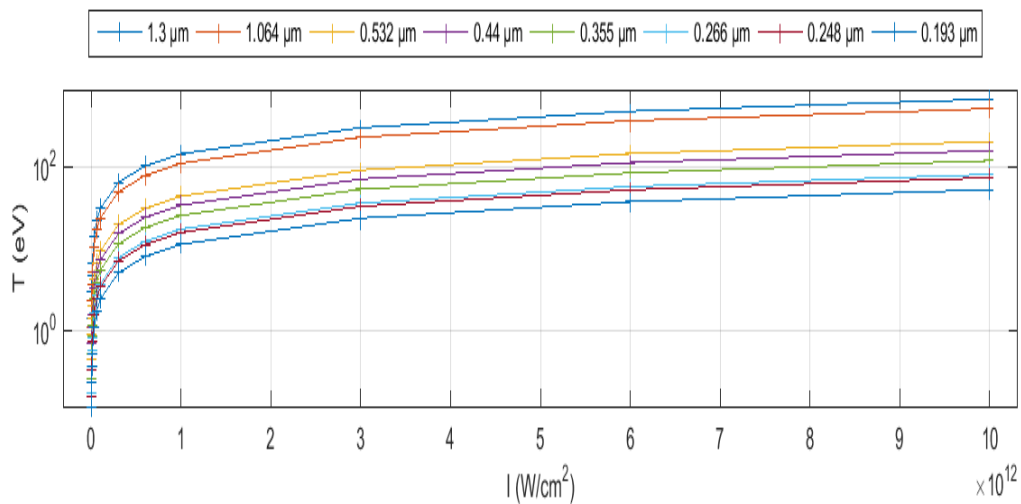


## 4.2 The Electron Temperature Deduced with Different Lasers and Different Intensities:

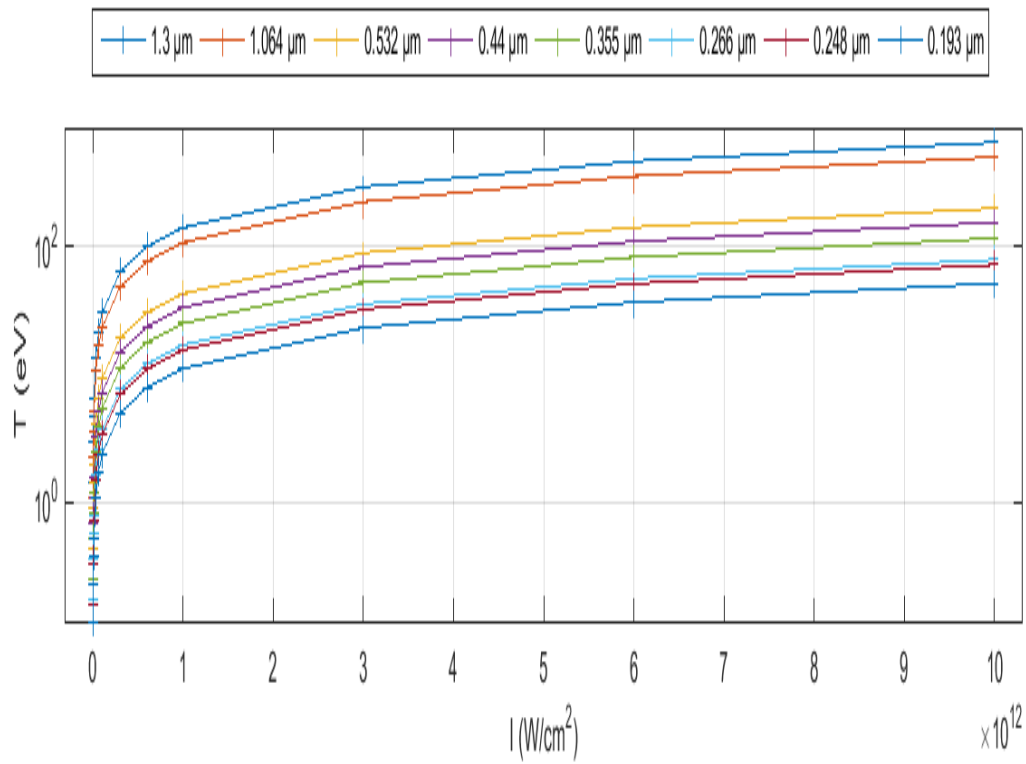
Fig (4-1) to fig (4-6) shows the relation between the electron temperatures for the alkaline earth group after irradiation by different types of lasers with the power densities.



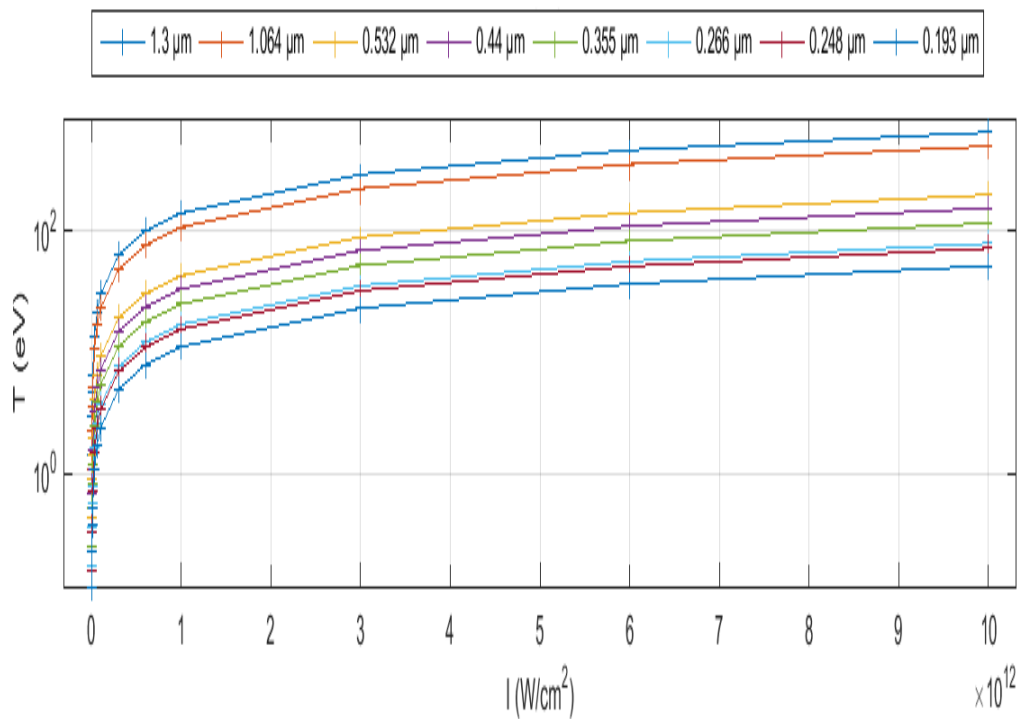
Fig(4-1): The relation between T(eV) of Be and lasers intensities( $W/cm^2$ )



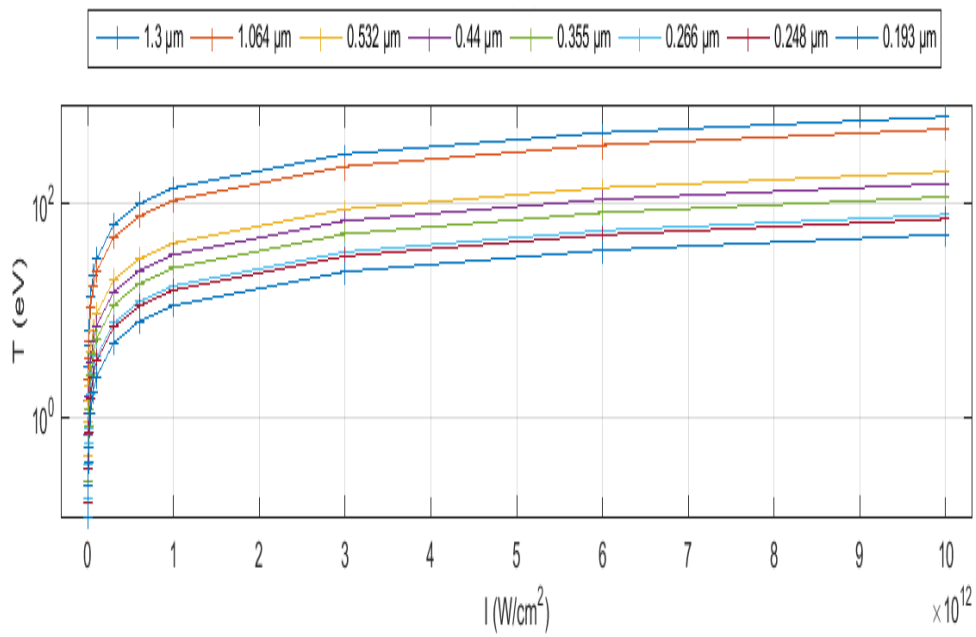
Fig(4-2): The relation between T(eV) of Mg and lasers intensities( $W/cm^2$ )



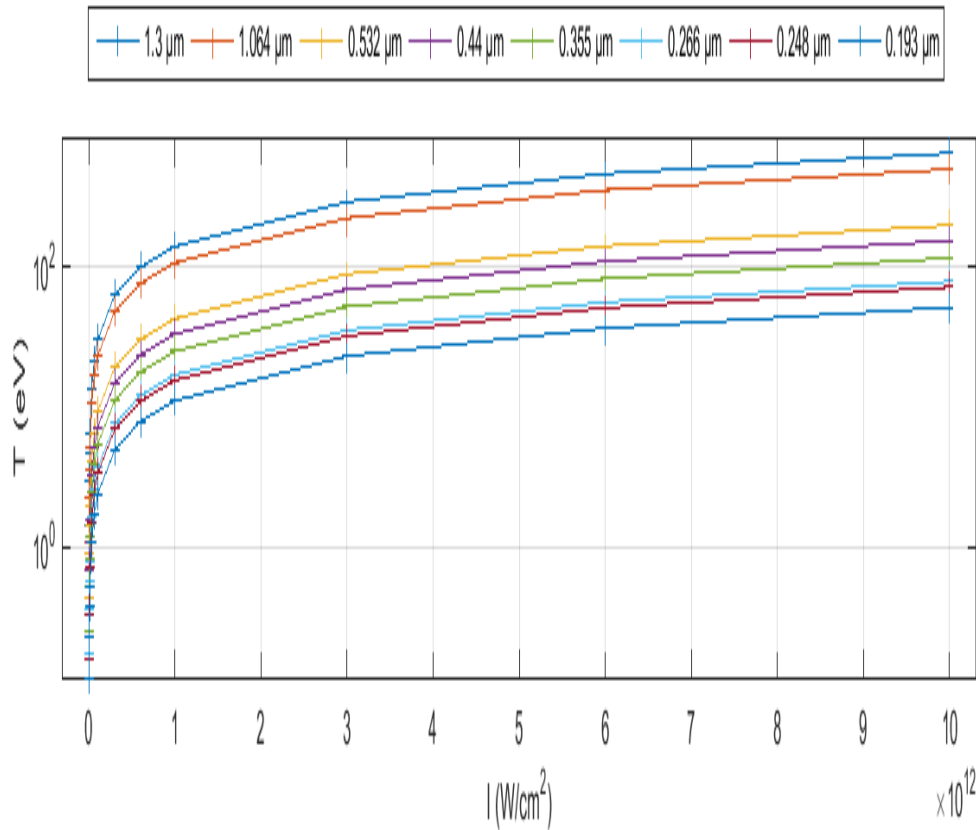
Fig(4-3): The relation between T(eV) of Ca and lasers intensities(W/cm<sup>2</sup>)



Fig(4-4): The relation between T(eV) of Sand lasersintensities(W/cm<sup>2</sup>)



Fig(4-5): The relation between  $T$ (eV) of Baand lasers intensities( $W/cm^2$ )



Fig(4-6): The relation between  $T$ (eV) of Ra and lasers intensities ( $W/cm^2$ )

### 4.3 The Relation between the Electron Temperature and Lasers Wavelengths:

Fig (4-7) to fig (4-12) shows the relations between the deduced electron temperature of the elements and the wavelengths served in this simulation work.

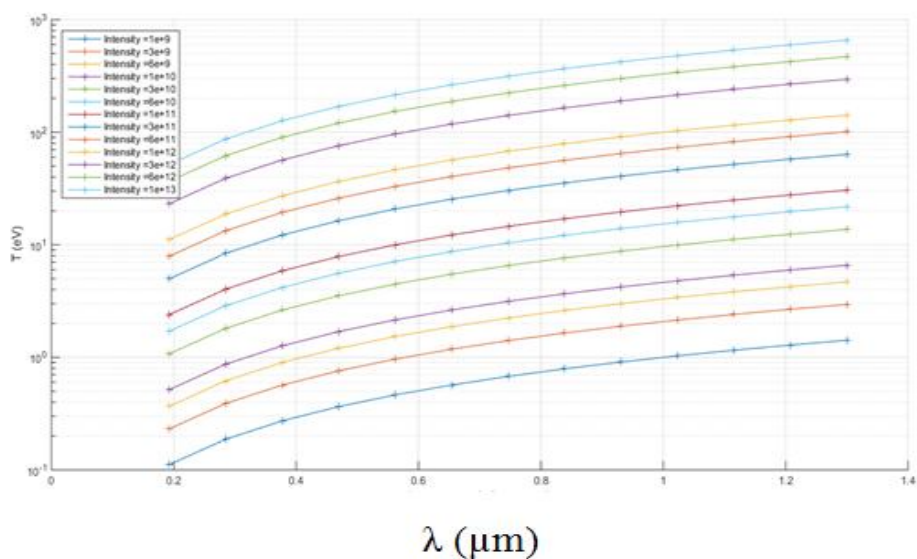


Fig (4-7):The relation between  $T$  (eV) of Beand lasers wavelengths ( $\mu\text{m}$ )

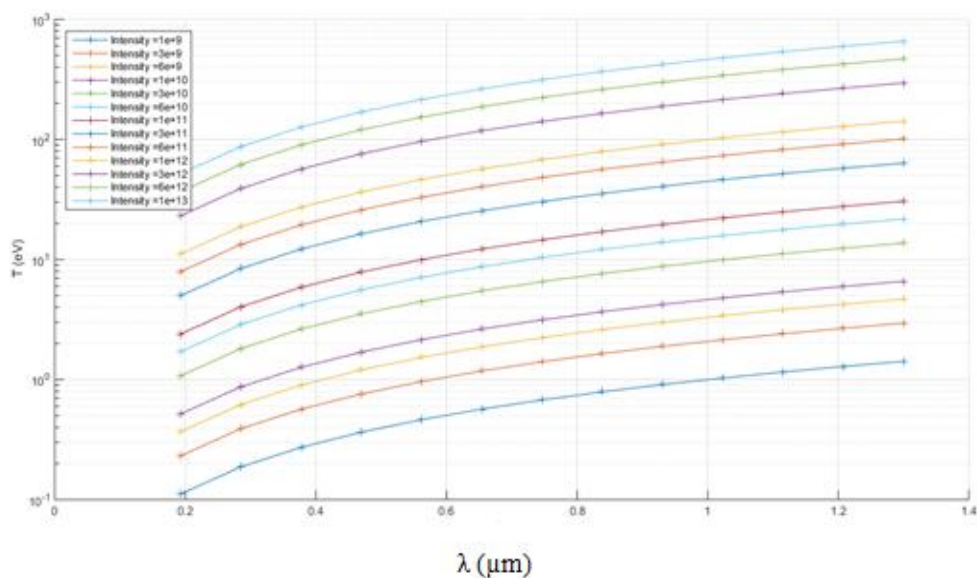
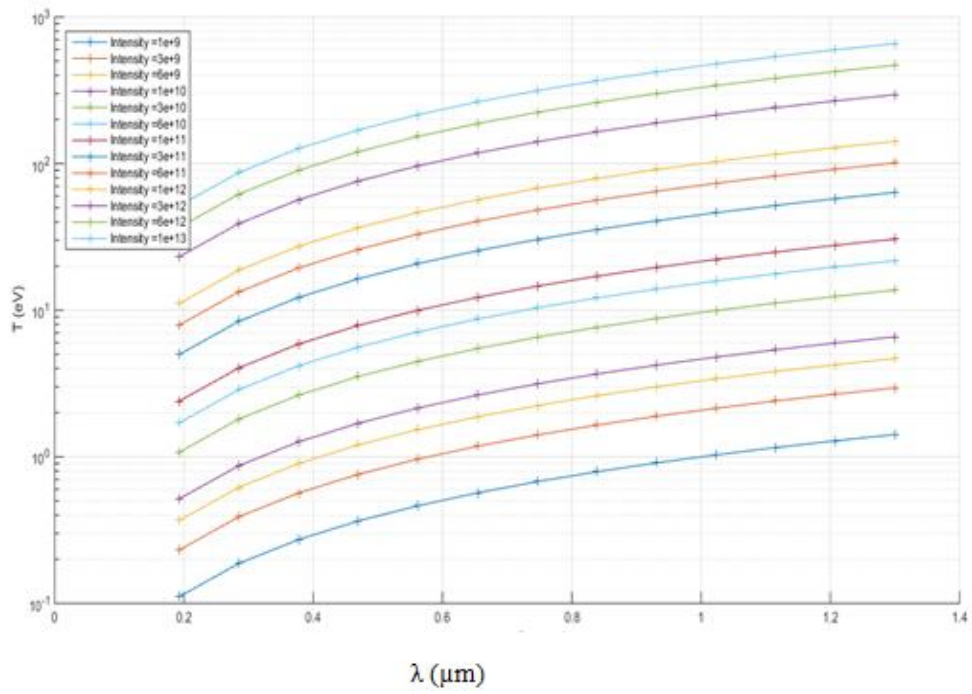
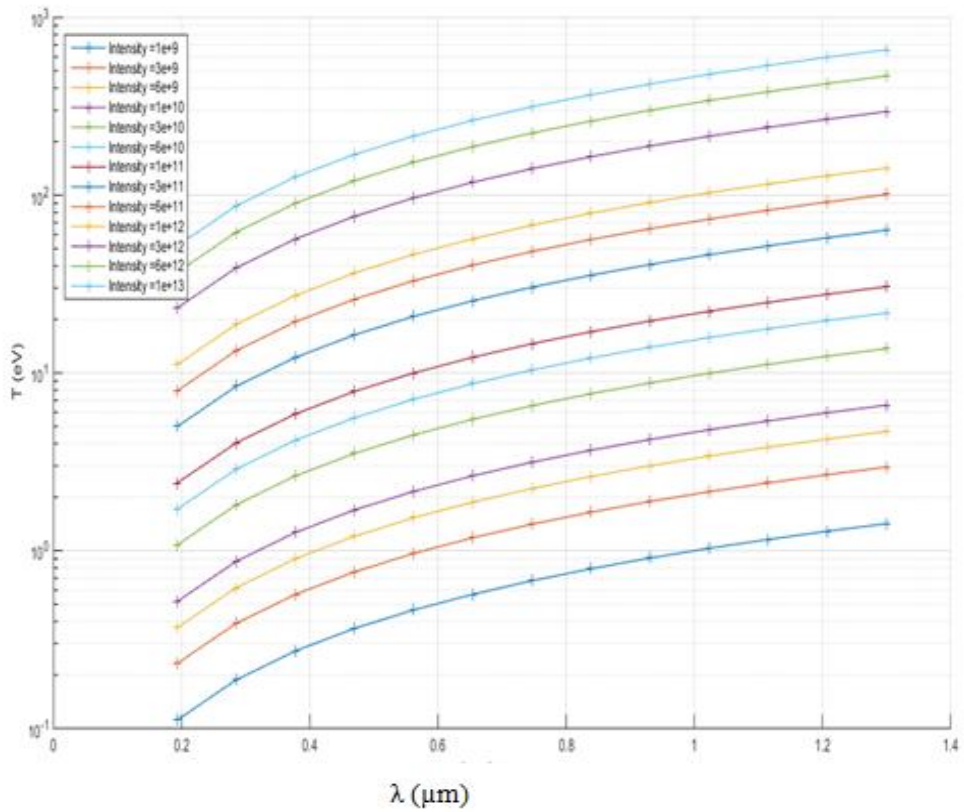


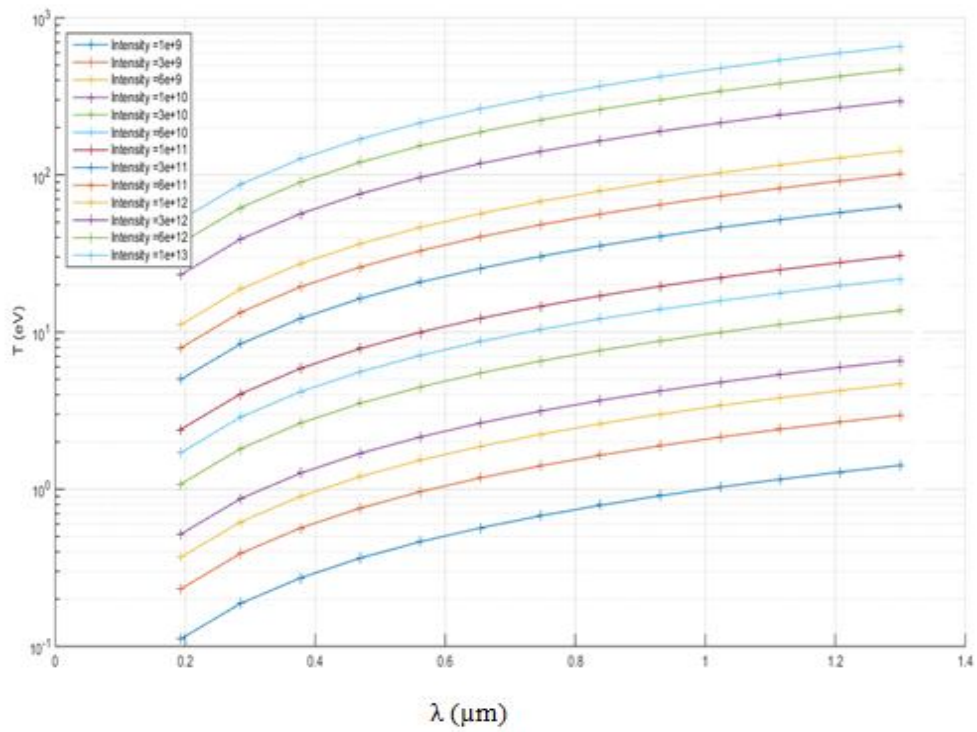
Fig (4-8): The relation between  $T$ (eV) of Mg and lasers wavelengths ( $\mu\text{m}$ )



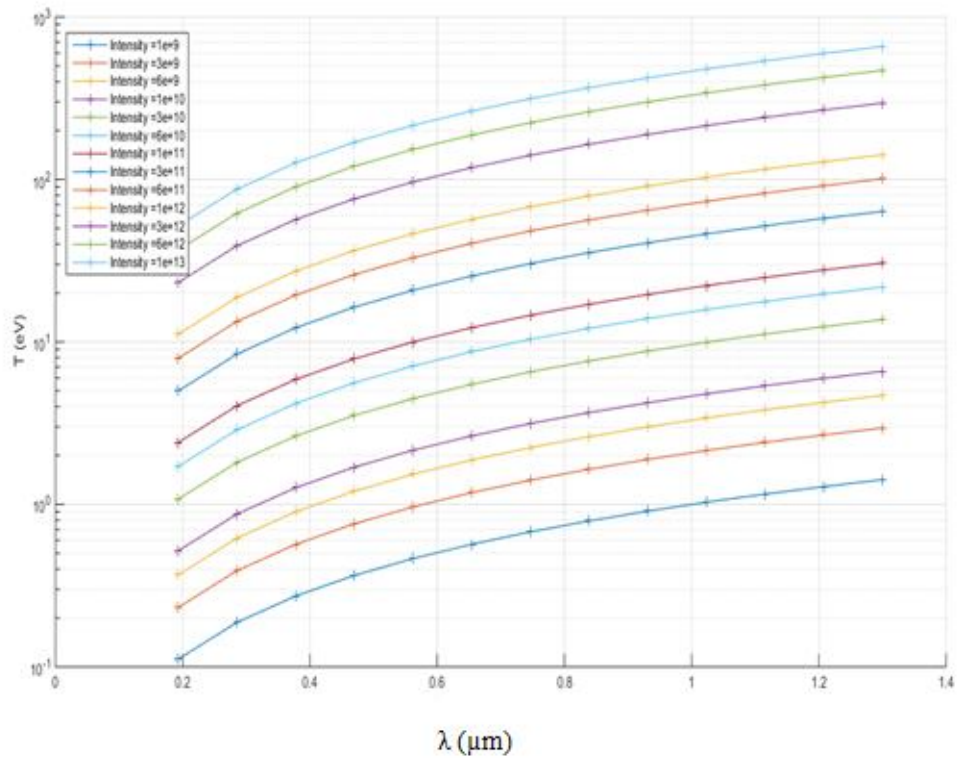
Fig(4-9):The relation between T(eV) of Ca and lasers wavelengths ( $\mu\text{m}$ )



Fig(4-10):The relation between T(eV) of Sr and lasers wavelengths ( $\mu\text{m}$ )



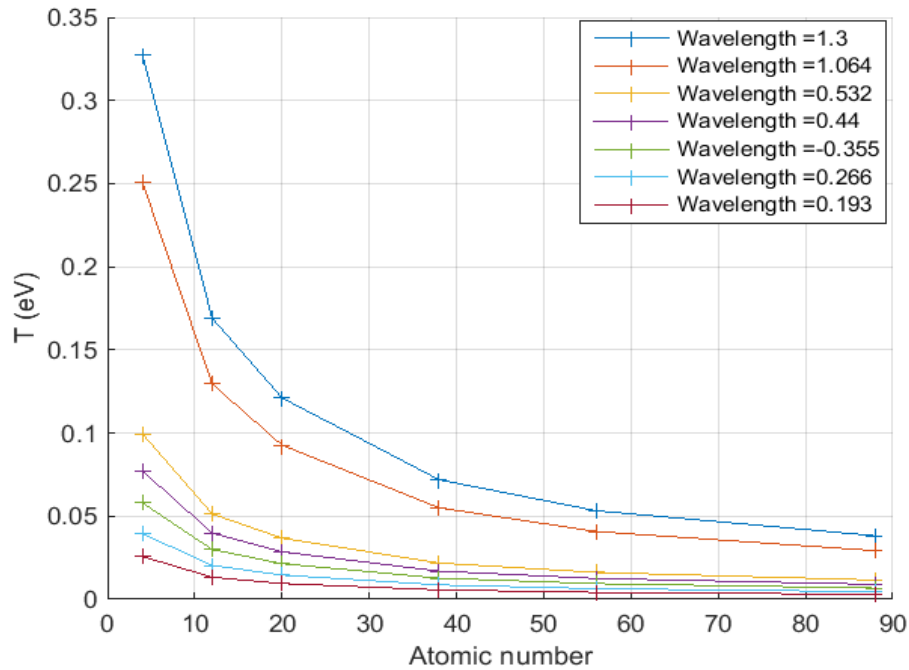
Fig(4-11):The relation between  $T$ (eV) of Ba and lasers wavelengths ( $\mu\text{m}$ )



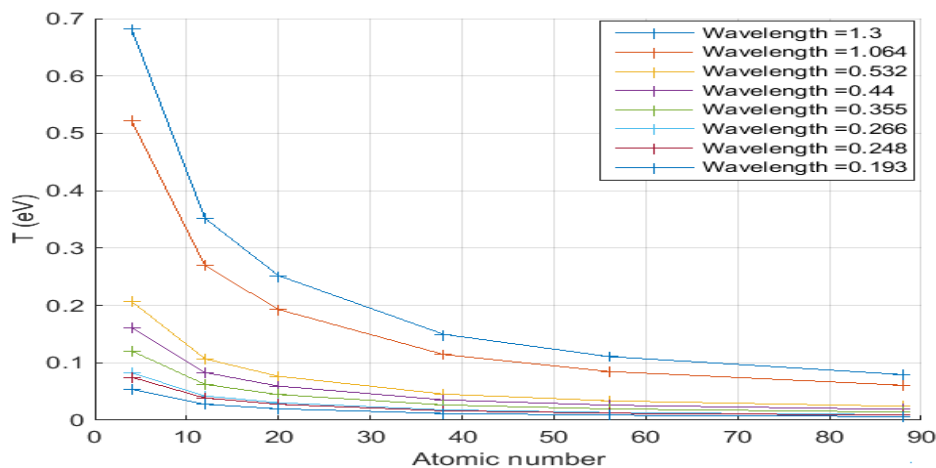
Fig(4-12):The relation between  $T$ (eV) of Ra and lasers wavelengths ( $\mu\text{m}$ )

#### 4.4 The Results of Electron Temperature Dependence on the Atomic Numbers (Z) of the Alkaline Earth Group:

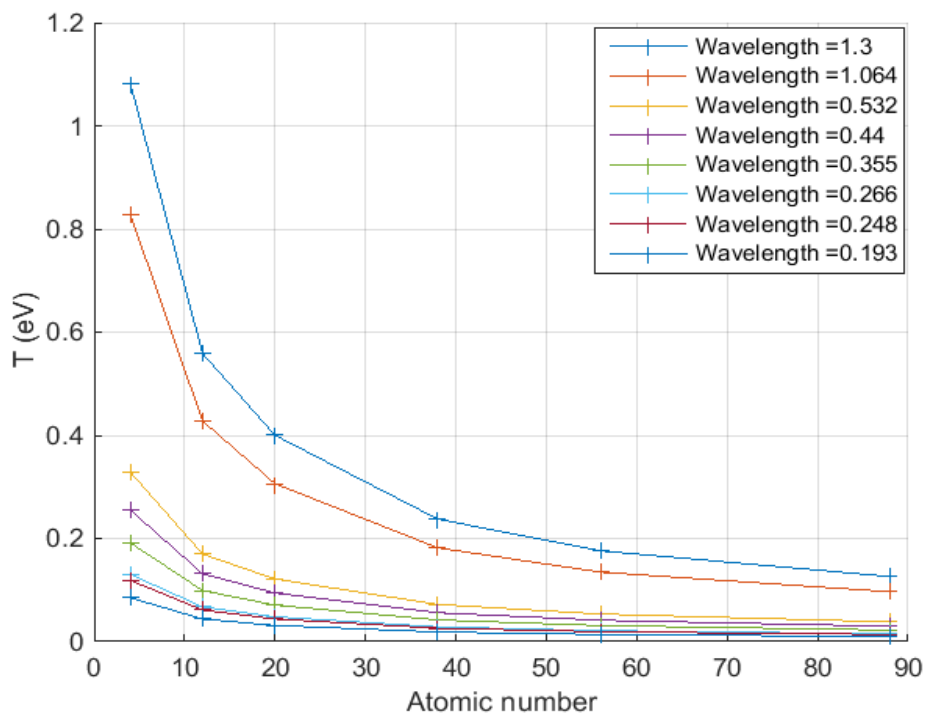
Figure(4-13) to fig(4-25) show the dependence of electron temperature on the atomic number of the alkaline earth elements irradiated with different lasers having power densities in the range from  $1 \times 10^9 \text{ w/cm}^2$  to  $1 \times 10^{13} \text{ w/cm}^2$ .



Fig(4-13):The relation between the electron temperature (eV) and the atomic numbers of the elements with different lasers at  $1 \times 10^9 \text{ (W/cm}^2)$

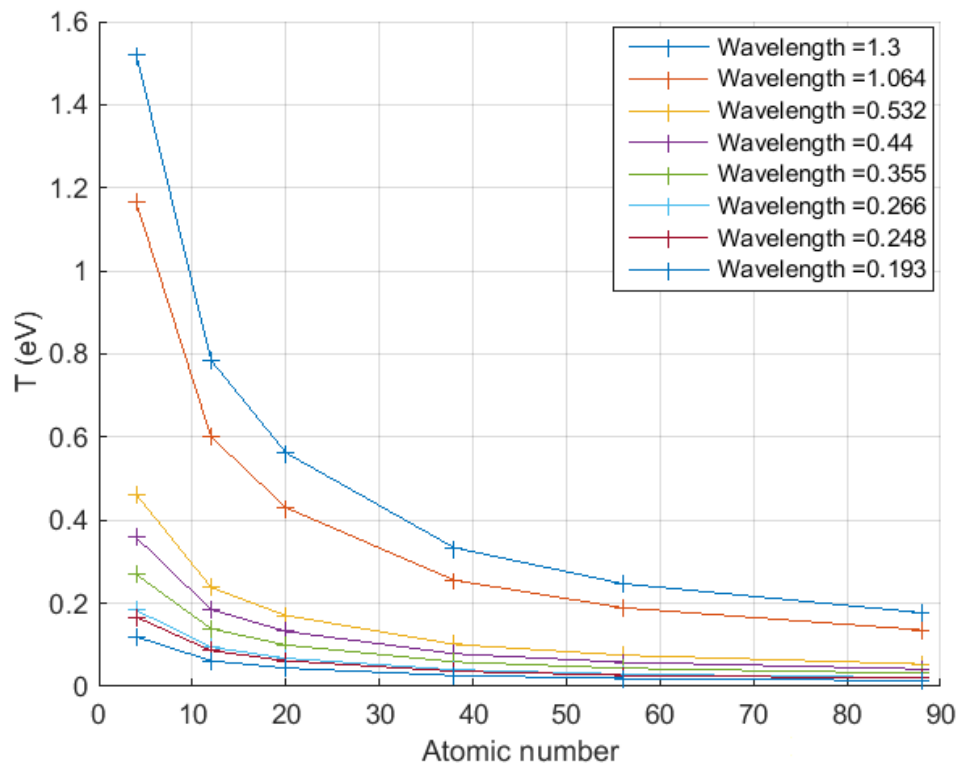


Fig(4-14):The relation between the electron temperature (eV)andtheatomic numbers of the elements with different lasers at $3 \times 10^9$ (W/cm<sup>2</sup>)

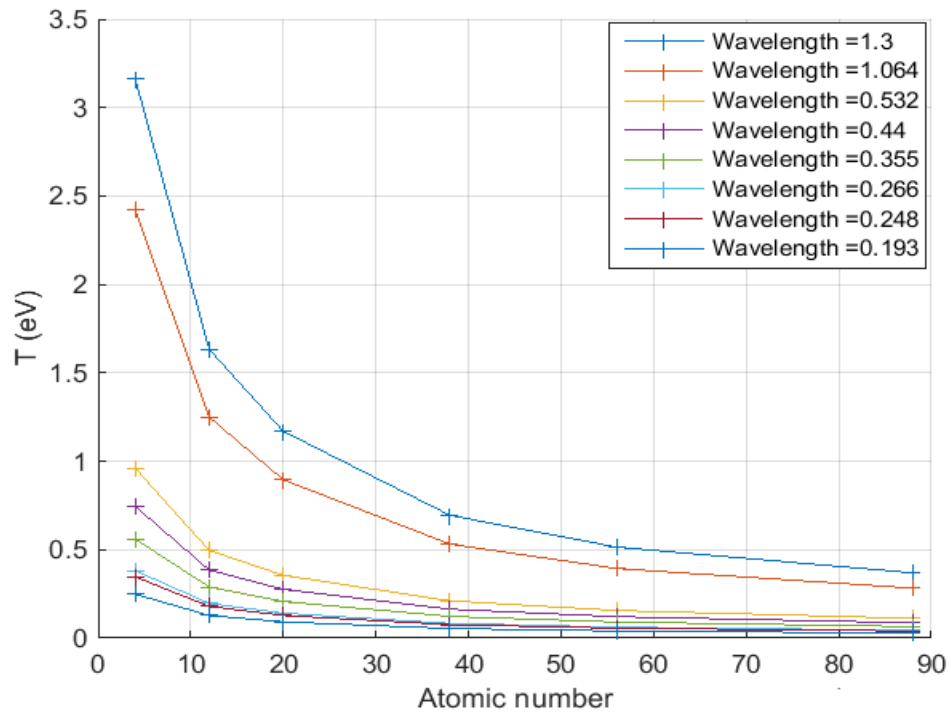


Fig(4-15):The relation between the electron temperature (eV)andtheatomic numbers of the elements with different lasers at $6 \times 10^9$ (W/cm<sup>2</sup>)

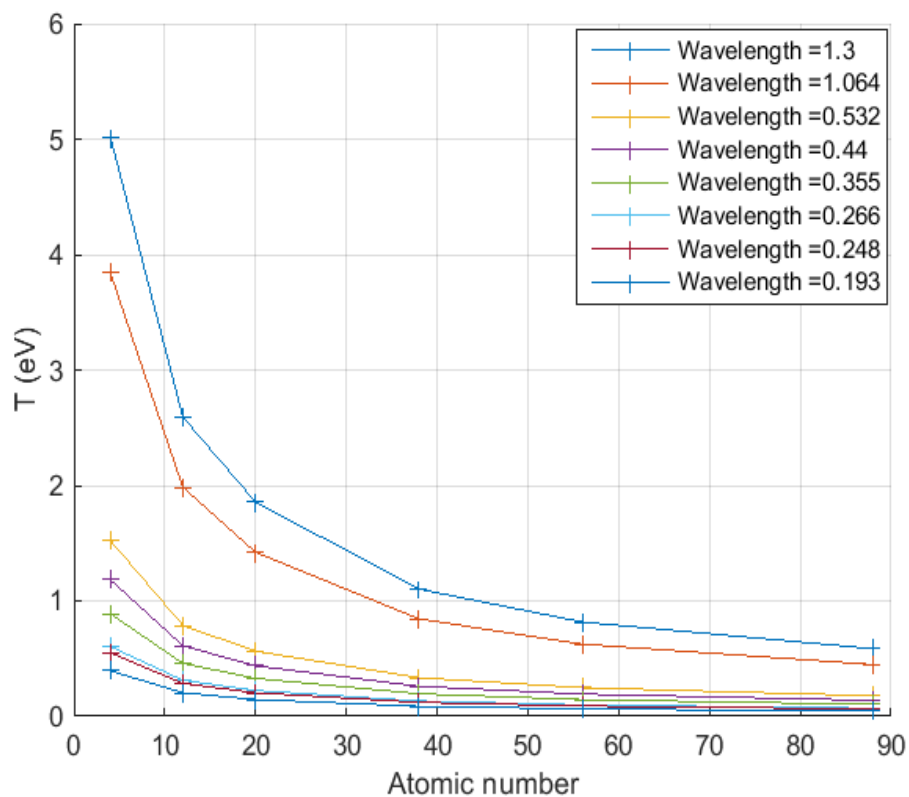




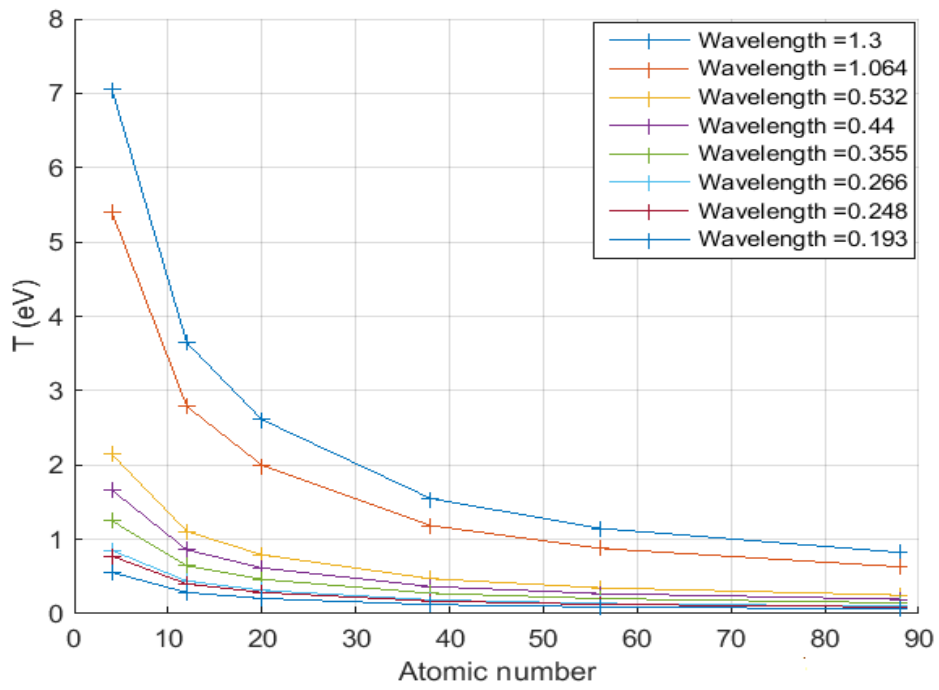
Fig(4-16):The relation between the electron temperature (eV) and the atomic numbers of the elements with different lasers at  $1 \times 10^{10} \text{ (W/cm}^2\text{)}$



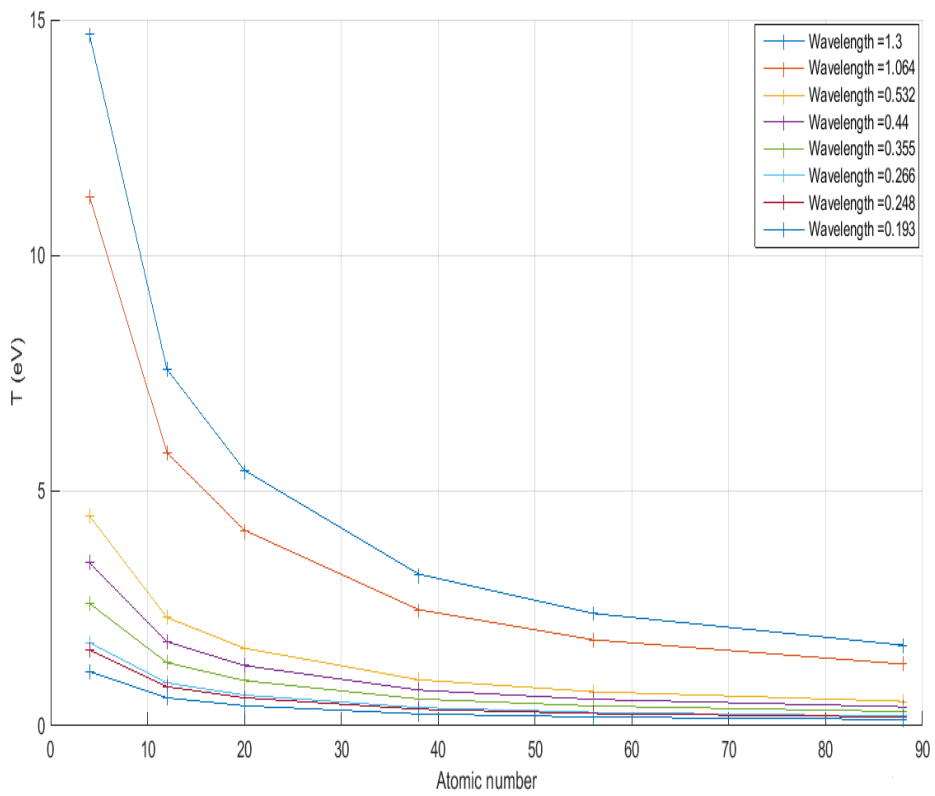
Fig(4-17):The relation between the electron temperature (eV)andtheatomicnumbers of the elements with different lasers at $3 \times 10^{10}(\text{W}/\text{cm}^2)$



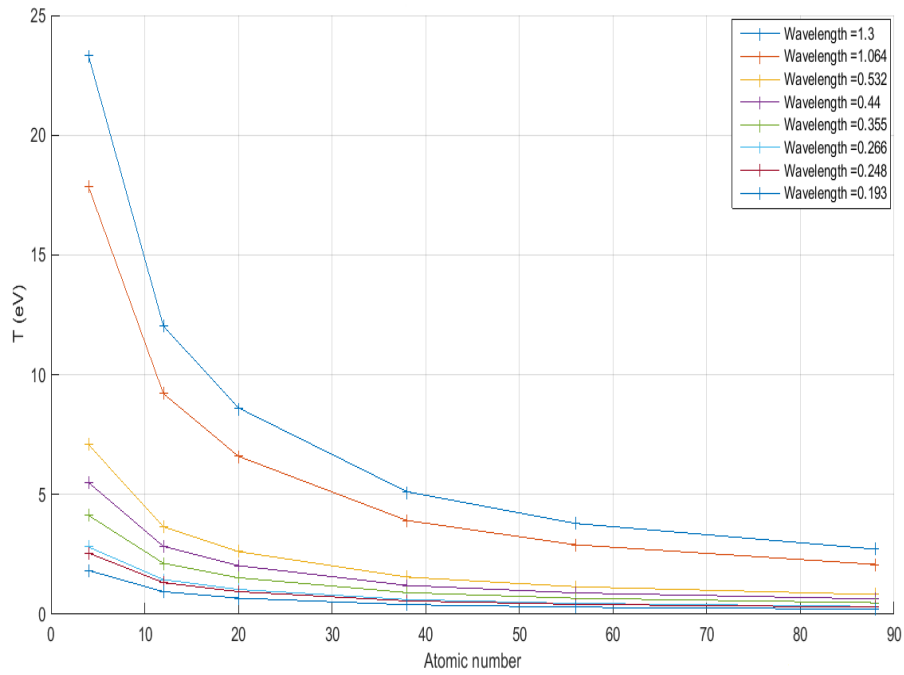
Fig(4-18): The relation between the electron temperature (eV)andtheatomic numbers of the elements with different lasers at $6 \times 10^{10}(\text{W}/\text{cm}^2)$



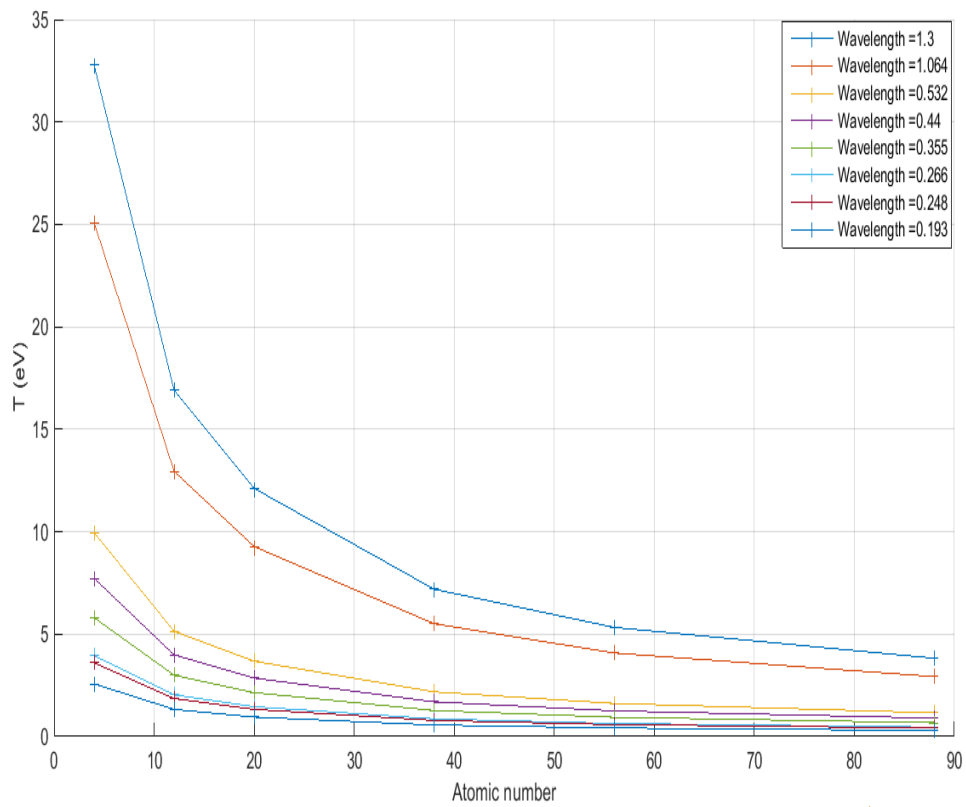
Fig(4-19):The relation between the electron temperature (eV)andtheatomic numbers of the elements with different lasers at $1 \times 10^{11} \text{ (W/cm}^2\text{)}$



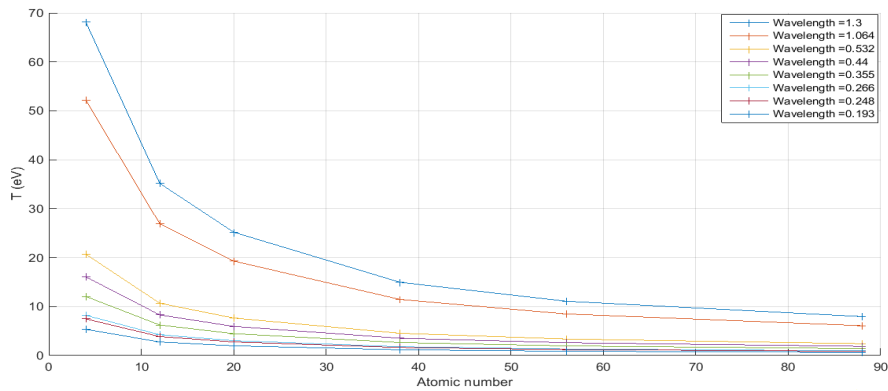
Fig(4-20):The relation between the electron temperature (eV)andtheatomic numbers of the elements with different lasers at $3 \times 10^{11}(\text{W}/\text{cm}^2)$



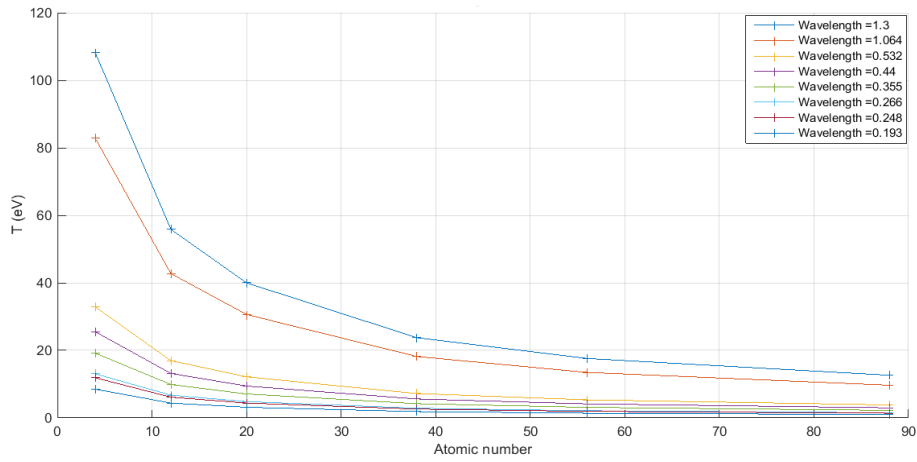
Fig(4-21):The relation between the electron temperature (eV)andtheatomic numbers of the elements with different lasers at $6 \times 10^{11}(\text{W}/\text{cm}^2)$



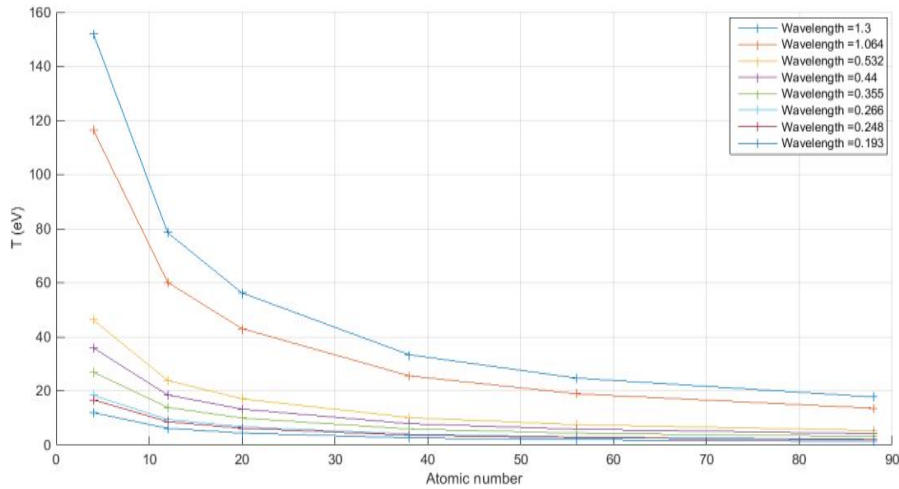
Fig(4-22):The relation between the electron temperature (eV)andtheatomic numbers of the elements with different lasers at $1 \times 10^{12} \text{ (W/cm}^2)$



Fig(4-23):The relation between the electron temperature (eV)andtheatomic numbers of the elements with different lasers at $3 \times 10^{12} \text{ (W/cm}^2)$



Fig(4-24):The relation between the electron temperature (eV)andtheatomic numbers of the elements with different lasers at  $6 \times 10^{12}(\text{W}/\text{cm}^2)$



Fig(4-25): The relation between the electron temperature (eV)andtheatomicnumbers of the elements with different lasers at  $1 \times 10^{13}(\text{W}/\text{cm}^2)$

## 4.5 The Discussion

The result of this simulation which was used to calculate the electron temperature was agreed with the results gained from experiments done in PALS (Prague Asterix Laser System) laboratory (Batani, 2007).

### 4.5.1 The Electron Temperatures Deduced with Different Lasers and Different Intensities:

For the electron temperature of alkaline earth plasma resulted from the irradiation by different laser wavelengths with different intensities, the results showed that when the laser intensity was increased the electron temperature increased. The nature and characteristics of the laser produced plasma strongly depend on the laser irradiance.

The results of this simulation are in agreement with the results of different work.

The reason behind increase of the electron plasma temperature is that when the target irradiated by laser, the vapour initially becomes slightly ionized, and absorbs part of the incident laser radiation. The energy is converted into internal energy of the plasma. With increase in plasma temperature, the degree of ionization of the vapour is also increased; thereby further enhancing the absorption of the incident laser radiation. As the plasma density and temperature rise, the vapour phase progressively behaves like an optically thick medium. The plasma effectively shields the target surface from the trailing part of the laser pulse. The energy in the plasma is then transferred away by thermal radiation or converted into hydrodynamic motion. Due to lateral expansion of the plasma, the energy radiated from the plasma to the target is often distributed over an area significantly larger than the laser beam spot (Harilal, 1997).

A radiating gas may be composed of molecules, atoms, ions and electrons. These particles have various energy levels associated with them. In accordance with the general scheme of allowed energy states of an atomic system, the electronic transitions accompanying absorption and emission of light are subdivided into three types: free-free, bound-free and bound-bound transitions. From an energy point of view on continuous spectra, bound-free and free-free transitions are of primary interest. The reason is that the radiant energy losses by distinct spectral lines usually represent small part of the continuous

spectrum. In this study it was assumed that the evaporated particles are either in atomic form or ionized states. In this relation the electron temperature was depended on the wavelength and intensity (Shaikh, et al., 2006).

#### **4.5.2 The Relation between the Electron Temperature and Lasers Wavelengths:**

In figures from [(4-7) to (4-12)], the relation between the electron temperature and power densities with different lasers was presented, when the wavelength of the laser was increased from 0.193  $\mu\text{m}$  to 1.3  $\mu\text{m}$  the electron temperature was increased. This result is agreed with the results of experiment for the measurement of electron density and temperature of a laser-induced zinc plasma experiment (Shaikh, et al., 2006), Nd-YAG laser was used in different wavelengths 1.064  $\mu\text{m}$ , and 0.532  $\mu\text{m}$ , 0.355  $\mu\text{m}$ , this experiment explained that when the laser wavelength was decreased from 1.064  $\mu\text{m}$  to 0.355  $\mu\text{m}$ , the temperature was decreased. Also there is an agreement of the simulation results with the result of the spectroscopic characterization of laser-ablated manganese sulfate plasma (Saliket. al 2014). The threshold for avalanche depends on the vapour ionization. Electrons will gain energy in the field through inverse Bremsstrahlung

absorption and lose energy by elastic and inelastic collisions with neutral particles. The electron temperature is higher with the Nd-YAG laser 1.064  $\mu\text{m}$  and Iodine laser 1.3  $\mu\text{m}$  compared to the case of lasers in the UV region 0.266  $\mu\text{m}$ , 0.248  $\mu\text{m}$ , 0.193  $\mu\text{m}$ , because the inverse Bremsstrahlung (IB) process is more efficient in the infrared region. Indeed the absorption coefficient is inversely proportional to  $\lambda^2$ . If the laser irradiance is high enough, primary electrons will gain energy larger than the ionization energy. These electrons will generate new



electrons by impact ionization of atoms of the vapour, thereby leading to cascade growth.

The IB absorption  $\alpha_{ib}$  via free electron is approximated from the expression:

$$\alpha_{ib}(\text{cm}^{-1}) = 1.37 \times 10^{-35} \lambda^3 N_e^2 T_e^{-1/2} \quad (4.1)$$

In this equation,  $\lambda$  is the wavelength of the photons in  $\mu\text{m}$ . As the incident laser energy is increased the longitudinal and lateral dimensions of this plasma are also increased. From equation (4.1) it is clear that IB is an efficient absorption process especially at the IR wavelengths. With increasing laser irradiance, more excited species, ions and free electrons are generated that interact with the incoming laser photon, leading to further heating and ionization and resulting in an increase in the absorption of the laser energy (Shaikh et al., 2006). The general outcome of the laser wavelength on the overall absorption in the plasma depends on the relative contribution of electron-ion (e-i) IB, electron-neutral (e-n) IB and PI (photoionization). The longer wavelength corresponds to lower photon energy and lower probability of PI from the excited levels, resulting in a lower PI absorption coefficient. In the case of shorter wavelengths, 0.355  $\mu\text{m}$ , 0.266  $\mu\text{m}$ , 0.248  $\mu\text{m}$ , and 0.193  $\mu\text{m}$ , lasers (e-n) IB and PI processes are dominant, because of the higher photon energy; therefore the contribution due to (e-i) IB is very small. Similarly with the 0.532  $\mu\text{m}$ , 0.44  $\mu\text{m}$  laser the (e-i) IB is larger than that of the 0.355  $\mu\text{m}$ , 0.266  $\mu\text{m}$ , 0.248  $\mu\text{m}$ , and 0.193  $\mu\text{m}$  lasers. One can conclude that at 1.3  $\mu\text{m}$  and 1.064  $\mu\text{m}$  laser the plasma absorption is entirely due to (e-i) IB (Harilal, 1997).

It is noted that the absorption due to inverse bremsstrahlung is negligibly small at low irradiance levels and increases exponentially with increasing laser irradiance.

In the case of the absorption via photoionization it can be estimated with Kramer's formula and the absorption coefficient is:

$$\alpha_{bi} = \sum_n 7.9 \times 10^{18} \left( \frac{E_n}{h\nu_1} \right)^3 \left( \frac{1}{E_n} \right)^{1/2} N_n \quad (4.2)$$

Where  $E_n$  and  $N_n$  are the ionization energy and number density of the excited state  $n$ ;  $h$  is Planck's constant,  $\nu_1$  is laser frequency;  $I$  is the ionization potential of the ground state atom. The absorption coefficient of photoionization is obtained by summing up all the excited states whose ionization energies are smaller than the laser photon energy (Chang and Warner, 1996).

The equation of the ionization rate in the case of photoionization is given by:

$$W_n = \omega_0 n_e^{3/2} \left( \frac{\xi_{os}}{I_{i_i}} \right)^P \quad (4.3)$$

where  $P = I_i / \hbar \omega_0$  is the number of photons absorbed and  $\xi_{os}$  is the electron oscillation energy which is given by:

$$\xi_{os} = 0.093 \lambda^2 I \text{ (eV)} \quad (4.4)$$

Where  $I$  is the power density used for the ablation ( $\text{W}/\text{cm}^2$ ) (G K et al., 1996).

Nevertheless, the amount of ablated matter is larger using an UV laser than with an IR laser.

#### **4.5.3 The Electron Temperature Dependence on the Atomic Numbers (Z):**

Infig (4-13) to fig (4-25), the relation between the electron temperature and the atomic number of the elements is presented. The electron temperature was decreased when the atomic numbers were increased at fixed intensity. The minimum laser intensity required for breakdown in the metal vapour and/or in the ambient gas is given by:

$$I_i(\text{MWcm}^{-2}) > 2 \times 10^3 \frac{\Delta}{\lambda^2 M} \quad (4.5)$$

where  $\Delta$  is the ionization potential of the neutral particles (in eV),  $\lambda$  in  $\mu\text{m}$  and  $M$  (amu) is the atomic mass (Boulrner–Leborgne et.al., 1993). This process is dominated by the inverse Bremsstrahlung process favoured for long laser wavelengths. The dependence of  $I_i$  with  $1/M$  means that it is easier to obtain a breakdown with a smallest atomic mass than larger atomic mass (Richter, 1990).

The basic principle of mass may be converted into energy and energy may be converted into mass. The conversion factor between mass and energy is huge, so that a small amount of mass produces a very large amount of energy (Elizer and Elizer, 2001).

## 4.6 Conclusions

From the obtained results one can conclude that:

1. The plasma electron temperature increased when the laser intensities was increased. The mathematical fitting is the 4th polynomial fitting.

2. Electron temperature increased with increasing the laser wavelength.
3. When the atomic number is increased the electron plasma temperature is decreased.

## 4.7 Recommendations

One can suggest the followings as future work

1. A practical measurement of the electron temperature for the same elements to compare the results with the results of this work.
2. Simulation of the nonlinear processes for the plasma of the same elements.
3. Using this program to calculate the electron temperature of other groups in periodic table.

## References

- Aliverdiev, A. and Batani, D. and Dezulian, R. and Vinci, T. (2011) 'Carbon equation of state at high pressure: the role of the radiative transport in the impedance mismatch diagnostics', *Nukleonika*; 56(2):165–169.

- Atzeni, S. (2004). *The physics of inertial fusion*, Clarendon Press- Oxford.
- Batani , D. and Strati, F. and Telaro, B. and L'ower, T. and Hall, T.andBenuzzi-Mounaix, A. and Koenig, M. (2003) 'Production of high quality shocks for equation of state experiments', *Eur. Phys. J. D* **23**, 99–107.
- Batani ,D. and Dezulian, R. and Stabile, H. and Tomasini, M. and Lucchini, G. and Canova ,F. and Redaelli, R. and Koenig ,M. and Benuzzi, A.and Nishimura ,H. and Ochi, Y. andUllschmied, J. andSkala, J. and Kralikova, B. and Pfeifer , M. andMocek, T. and Präg, A. and Hall, T. and Milani,P. and Barborini, E. and Piser, P. (2007) 'High Pressure Laser-Generated Shocks and Application to EOS of Carbon', *IOP Publishing Ltd*
- Batani, D. and Baton, S. (2011) 'Laser-Plasma Interaction and Target Coupling in the Intensity Regime relevant for Shock-Ignition', *International Workshop on ICF Shock Ignition*, Rochester, NY.
- Batani, D. and Dezulian, r. and Redaelli, r. and Benocci, r. and Stabile, h.and Canova ,f. and Desai ,t. and Lucchini, g. and Krousky, e. and Masek, k. and Pfeifer, m. and Skala, j. and r. and Dudzak and Rus. b. and Ullschmied, j. and Malka, v. and Faure, j. and .Koenig, m. and Limpouch, j. and Nazarov, w. and Pepler, D. and Nagai ,k. and Norimatsu, t. and Nishimura, h. (2006) 'Recent experiments on the hydrodynamics of laser-produced plasmas conducted at the PALS laboratory',*Laser And Particle Beams* ,Cambridge University Press 0263-0346.
- Bellan, M., P. (2004) *Fundamentals of Plasma Physics*,Published by CUP.

- Benuzzi ,A. and Loewer, T. and Koenig, M. F., Bernard and Batani ,D. and Daniele ,B. D., C. and P., D. (1996) ‘indirect and direct laser driven shock waves and applications to copper equation of state measurements in the  $10^{-40}$  Mbar pressure range’, *Physical Review E* Volume 54, Number 2 August 1996.
- Boulanger-Leborgne ,C. and Herrmann, J. and Dubreuil, B. (1993) ‘Plasma formation resulting from the interaction of a laser beam with a solid metal target in an ambient gas’, *Plasma Sour, Sci. Tec*, 2 219.
- Boustie,M. and Berthe, L. and D , t. and Arrigoni ,M (2008) ‘laser shock waves: fundamentals and applications’, *1st international symposium on laser ultrasonics: science, technology and applications* July 16-18 2008, montreal, canada
- Burdiak, G. C. (2014) *Cylindrical Liner Z-pinches as Drivers for Converging Strong Shock Experiments*, PhD thesis, Springer International Publishing Switzerland, Imperial College London, UK.
- Campos ,D., D. (2010) *Emission Characteristics Of Nd:Yag And Co<sub>2</sub> Laser-Produced Tin Plasmas For Extreme Ultraviolet Lithography Source Development*, master thesis , Purdue University.
- Chang,J. J.and Warner, B. E. (1996) ‘Laser-plasma interaction during visible-laser ablation of methods’,*Appl. Phys.Lett.* **69**, 473.
- Chen, E., F. (1984) *Introduction to Plasma Physics and Controlled Fusion*, vol 1 (Plenum).
- Cremers, D. A. and Radziemski, L . J. (2013) *Handbook of Laser-Induced Breakdown Spectroscopy*, John Wiley & Sons, Ltd.

- Dardis, J. (2009) *Interactions of Intense Optical and Extreme – Ultra Violet lasers with atoms and solids*, PhD thesis, Dublin City University.
- De Rességuier ,T. and Loison, D.and Dragon, A. and Lescoute ,E. (2014). ‘Laser Driven Compression to Investigate Shock-Induced Melting of Metals’, *Journal of metals*,30 October, and [www.mdpi.com/journal/metals/](http://www.mdpi.com/journal/metals/).
- Dendy,O.,R. (1993) *Plasma Physics An Introductory Course*, Cambridge University Press, 323-324.
- Dhareshwar , J. , L. and A, Naik, P. and Kaushik, C., T. and Pant ,C.,H.(1992) ‘Laser Driven Shock wave Studies in Gold Coated Plexiglas Targets’, *Taylor & Francis*, 10:5-6, 695-706,
- Eliezer, S. (2002). *The Interaction of High-Power Lasers with Plasmas*, IOP Publishing Ltd.
- Eliezer, S. and A., Ghatak and H., Hora (1986).*An Introduction to Equations of State: Theory and Applications*, Cambridge: Cambridge University Press.
- Eliezer, S. and Eliezer, Y. (2001). *The Fourth State of Matter*, IOP Publishing Ltd.
- Eliezer, S. and Ghatak , A. and Hora, H. (1986) *Fundamentals of Equations of State*, World Scientific Singapore.
- Fridman and A., Alexander and Kennedy, and Lawrence, A. (2004) *Plasma Physics and Engineering*, Taylor & Francis Routledge.
- G K ,Varier, , and R. C., Issacand Harial,S. and Bindhu,V. C. and Nampoori,N.,P.,V. and C.,P.,G., Vallabhan (1996). Investigation on nanosecond laser produced plasma in air from the multi-component material  $\text{YBa}_2\text{Cu}_3\text{O}_7$ , *Elsvier* ,657-666
- Geohegan , B. , D. and Puretzky, A., A. (1996) ‘Laser ablation plume thermalization dynamics in background

gases:combined imaging,optical absorption and emission spectroscopy, and ion probe measurements' , *Appl. Sur. Sci.* 96-98 126.

- Giulietti, D. and Gizzi, Le. A. (1998) *X-Ray Emission from Laser Produced Plasmas*, PhD thesis Dipartimento di Fisica, Università di Pisa, Piazza Torricelli, n.2, 56100, Pisa, Italy.
- Grades, d., E. (2008) *Bremsstrahlung in Dense Plasmas: A Many-Body Theoretical Approach*, PhD thesis ,Universit at Rostock.
- Gizzi, A. ,L. (1994) *Characterization of Plasma Produced by Picosecond and nanosecond Laser Pulses*,PhD thesis .University of London
- H, Griem. (1964) *Plasma Spectroscopy*, (McGraw-Hill).
- Hall, M., I. (2006) *Experimental and Computational K-shell Spectroscopy of Laser Produced Plasma*, PhD thesis, University of York.
- Harilal, S., S. (1997)*Optical Emission Diagnostics of Laser Produced Plasma from  $YBa_2Cu_3O_7$* , PhD thesis, *Laser Division International School Of Photonics Cochin University Of Science And Technology Cochin - 682 022, India.*
- Harilal, S., S. and Bindhu, V., C. and Issac, R. C. and Nampoori, N., P. and Vallabhan, G., P., C. (1997) 'Electron density and temperature measurements in a laser produced carbon plasma', *American Institute of Physics*, S0021-8979(97)04116-9.
- Hitz, B. and. Ewing, J., J. and Hecht, J. (2001) *Introduction to Laser Technology*, Wiley.
- Hoigh, P. (2010) '*Laser optical, Optical and Electrical Diagnostics of Colliding Laser Produced Plasmas*', PhD thesis, Dublin City University.



- Inan, U. and Golkowski, M.(2011) *Principles of Plasma Physics for Engineers and Scientists*, Cambridge University Press.
- John D., L. (1995) ‘Development of the indirect-drive approach to inertial confinement fusion and the target physics basis for ignition and gain’, *Phys. Plasmas* 2, 3933– 4024.
- Kikuchi, M. and Lackner, K. and Quang, T.,M.(2012) *Fusion Physics*, IAEA,Austria.
- Krall, N. A. and W, Trivelpiece A. (1973) *Principle of Plasma physics*, McGraw-Hill, Inc.
- Leite, P., E. (2010) *Matlab - Modelling, Programming and Simulations*,Sciyo,www.sciyo.com.
- Macchi, A. (2013) *A Superintense Laser–Plasma Interaction Theory Primer*, Springer Dordrecht Heidelberg New York London.
- Magyar, J., R. and Mattsson, R., T. (2013) ‘Mixing of equations of state for xenon-deuterium using density functional theory’,*Phys. Plasmas*, 20, 032701.
- McKenna, P. and Neely, D. and Bingham, R. and A., Dino, J.(2013). *Laser-Plasma Interactions and Applications*, Springer Switzerland Heidelberg New York Dordrecht London
- Mora, P. (1982) ‘Theoretical model of absorption of laser light by a plasma’, *physics Fluids*,*AIP Publishing*,25, 1051
- Muraoka,K.and Maeda,M.(1993)Application of laser-induced fluorescence to high-temperature plasmas, *Plasma. Phys. Control. Fusion* 35 633.
- Muraoka, K. and Maeda, M. (2001) *Laser-Aided Diagnostics of Plasmas and Gases*, IOP Publishing Ltd.
- Musazzi, S. and Perini, U. (2014) *Laser-Induced Breakdown Spectroscopy*, Springer-Verlag Berlin Heidelberg.

- Osman, A., M. (2011) *Diagnostics of electron Temperature in Laser Produced Plasma and determination of its Effect on Some Deposited Films Properties*, PhD thesis, Sudan University.
- Ozaki, N. and A, K. and Ono ,T. and Shigemori ,K. and Nakai, M. and Azechi ,H. and Yamanaka, T. and Wakabayashi ,K. and Yoshida, M. and Nagao, H. and Kondo, K. (2004) ‘Characterization of GEKKO/HIPER-Driven Shock Waves for Equation-of-State Experiments in Ultra-High-Pressure Regime’, *Physics of Plasmas*, Volume 11, Number 4.
- Pant, C., H. and Shukla, M. and Senecha, K., V. and Bandyopadhyay , S. and Rai, N., V. and Khare, P. and Bhat, K.,R. and Godwal, K., B. and Gupta, K., N. (2002) ‘Equation-of-state studies using laser-driven shock wave propagation through layered foil targets’, *Current science*, vol. 82, no. 2, 25 January 2002.
- Peratt, A. L. (2015) *Physics of the Plasma Universe*, Second edition, Springer Science+ Business Media New York.
- Piel, A. (2010) *Plasma Physics*, Springer-Verlag Berlin Heidelberg Dordrecht London New York.
- Richter, A. (1990) ‘Characteristic features of laser-produced plasmas for thin film deposition’, *Elsevier B.V.* **188** 275.
- Salik , M. and Hanif, M. and Wang, J. and Zhang , Q., X. (2014) Spectroscopic characterization of laser-ablated manganese sulfate plasma, *Cambridge University Press* , [Laser and Particle Beams](#) / Volume 32 / Issue 01 , pp 137-144.
- Salzmann, D. (1998) *Atomic Physics in Hot Plasmas*, Oxford University Press, New York.
- Schweitzer, M .J . (2008) *Numerical Simulation of Relativistic Laser-Plasma Interaction*, PhD theses, Universit“ at D“usseldorf.

- Shaikh , M. , N. and Rashid , B. and Hafeez, S. and Jamil ,Y. and Baig ,A.,M. (2006) ‘Measurement of electron density and temperature of a laser-induced zinc plasma’, *J. Phys. D: Appl. Phys.* **39** ,1384–1391.
- Singh, J.P. and Thakur, S.N. (2007) *Laser Induced Breakdown spectroscopy*, Elsevier.
- Swanson, D. G (2003) *Plasma Waves*, 2nd Edition. IOP Publishing Ltd.
- Temporal ,M. and Atzeni, S. and Batani, D. and Koenig, M. and Benuzzi, A. and Faral ,B(1997) ‘Numerical simulations for the design of absolute equation-of-state measurements by laser-driven shock waves’, *Il NuovoCimento*, Vol. 19 D, N. 12
- Y, ELİF. (2006) *Theoretical Investigation of Laser Produced Plasma Ni- like Sn Plasma*, Master’s thesis, Middle East technical university, viewed September 2006.
- Zhang, Z. and Han. ,Zhen-Xue., and. Dulikravich ,G.S. (2001) ‘Numerical simulation of laser induced plasma during pulsed laser deposition’, *journal of applied physics*, volume 90, number 12